


Article

Structure-Activity Relationships of Holothuroid's Triterpene Glycosides and Some In Silico Insights Obtained by Molecular Dynamics Study on the Mechanisms of Their Membranolytic Action

Elena A. Zelepuga , Alexandra S. Silchenko, Sergey A. Avilov and Vladimir I. Kalinin *

G.B. Elyakov Pacific Institute of Bioorganic Chemistry, Far Eastern Branch of the Russian Academy of Sciences, Pr. 100-letya Vladivostoka 159, Vladivostok 690022, Russia; zel@piboc.dvo.ru (E.A.Z.); silchenko_als@piboc.dvo.ru (A.S.S.); avilov_sa@piboc.dvo.ru (S.A.A.)
* Correspondence: kalininv@piboc.dvo.ru; Tel./Fax: +7-(423)2-31-40-50

Abstract: The article describes the structure-activity relationships (SAR) for a broad series of sea cucumber glycosides on different tumor cell lines and erythrocytes, and an in silico modulation of the interaction of selected glycosides from the sea cucumber *Eupentacta fraudatrix* with model erythrocyte membranes using full-atom molecular dynamics (MD) simulations. The in silico approach revealed that the glycosides bound to the membrane surface mainly through hydrophobic interactions and hydrogen bonds. The mode of such interactions depends on the aglycone structure, including the side chain structural peculiarities, and varies to a great extent. Two different mechanisms of glycoside/membrane interactions were discovered. The first one was realized through the pore formation (by cucumariosides A₁ (**40**) and A₈ (**44**)), preceded by bonding of the glycosides with membrane sphingomyelin, phospholipids, and cholesterol. Noncovalent intermolecular interactions inside multimolecular membrane complexes and their stoichiometry differed for **40** and **44**. The second mechanism was realized by cucumarioside A₂ (**59**) through the formation of phospholipid and cholesterol clusters in the outer and inner membrane leaflets, correspondingly. Noticeably, the glycoside/phospholipid interactions were more favorable compared to the glycoside/cholesterol interactions, but the glycoside possessed an agglomerating action towards the cholesterol molecules from the inner membrane leaflet. In silico simulations of the interactions of cucumarioside A₇ (**45**) with model membrane demonstrated only slight interactions with phospholipid polar heads and the absence of glycoside/cholesterol interactions. This fact correlated well with very low experimental hemolytic activity of this substance. The observed peculiarities of membranotropic action are in good agreement with the corresponding experimental data on hemolytic activity of the investigated compounds in vitro.

Keywords: triterpene glycosides; sea cucumber; membranolytic action; hemolytic; cytotoxic activity; molecular dynamic simulation



Citation: Zelepuga, E.A.; Silchenko, A.S.; Avilov, S.A.; Kalinin, V.I. Structure-Activity Relationships of Holothuroid's Triterpene Glycosides and Some In Silico Insights Obtained by Molecular Dynamics Study on the Mechanisms of Their Membranolytic Action. *Mar. Drugs* **2021**, *19*, 604. <https://doi.org/10.3390/md19110604>

Academic Editor: Vassilios Roussis

Received: 27 September 2021

Accepted: 20 October 2021

Published: 25 October 2021

Publisher's Note: MDPI stays neutral with regard to jurisdictional claims in published maps and institutional affiliations.



Copyright: © 2021 by the authors. Licensee MDPI, Basel, Switzerland. This article is an open access article distributed under the terms and conditions of the Creative Commons Attribution (CC BY) license (<https://creativecommons.org/licenses/by/4.0/>).

1. Introduction

The majority of triterpene glycosides from sea cucumbers possess strong hemolytic and cytotoxic actions against different cells, including cancer cells [1–4]. However, the mechanism of their membranolytic action is not yet fully understood at the molecular level, particularly in relation to the structural diversity of these compounds. Some trends of SAR of sea cucumber glycosides have been discussed [5,6], but the molecular interactions of different functional groups with the components of biomembranes which affect the membranotropic action of the glycosides remain unexplored.

The broad spectrum of bioactivity of sea cucumber triterpene glycosides derives from their ability to interact with the lipid constituents of the membrane bilayer, changing the

functional properties of the plasmatic membrane. Sterols are very important structural components influencing the properties and functions of eukaryotic cell membranes. The selective bonding to the sterols of the cell membranes underlines the molecular mechanisms of action of many natural toxins, including triterpene glycosides of the sea cucumbers. The formation of complexes with 5,6-unsaturated sterols of target cell membranes is the basis of their biological activity including ichthyotoxic action that may protect sea cucumbers against fish predation. In fact, some experimental data indicated the interaction of the aglycone part of the glycosides with cholesterol [7,8]. The saturation of ascites cell membranes with cholesterol increased the cytotoxicity of the sea cucumber glycosides [9]. This complexing reaction of both the animal and plant saponins leads to the formation of pores, the permeabilization of cells, and in the case of red blood cells for which the membranes are known to be enriched in cholesterol [10], the subsequent loss of hemoglobin in the extracellular medium [11]. Malyarenko et al. tested a series of triterpene glycosides isolated from the starfish *Solaster pacificus* that had exogenic origin from a sea cucumber eaten by this starfish [12]. The authors showed that the addition of cholesterol to corresponding tumor cell culture media significantly decreases the cytotoxicity of these glycosides. It clearly confirmed the cholesterol-dependent character of the membranolytic action of sea cucumber triterpene glycosides. It is of special interest that the activity of a glycoside with 18(16)-lactone instead of 18(20)-lactone, and a shortened side chain, was also decreased by the adding of cholesterol.

The sea cucumber glycosides may be active in subtoxic concentrations, and such a kind of activity is cholesterol-independent. Aminin et al. showed that the immunostimulatory action of cucumarioside A₂-2 from *Cucumaria japonica* resulted from the specific interaction of the glycoside with a P2X receptor and was cholesterol-independent [13]. The addition of cholesterol to the medium or to the mixture of substances may decrease the cytotoxic properties of the glycosides while preserving their other activities. This property of cholesterol has been applied to the development of ISCOMs (immune-stimulating complexes) and subunit protein antigen-carriers, composed of cholesterol, phospholipid, and glycosides [14,15]. Moreover, the immunomodulatory lead—“Cumaside” as a complex of monosulfated glycosides of the Far Eastern Sea cucumber *Cucumaria japonica* with cholesterol, has been created [16]. It possesses significantly less cytotoxic activity against sea urchin embryos and Ehrlich carcinoma cells than the corresponding glycosides, but has an antitumor activity against different forms of experimental mouse Ehrlich carcinoma in vivo [17].

Therefore, cholesterol seems to be the main molecular target for the majority of glycosides in the cell membranes. However, the experimental data for some plant saponins indicate that saponin-membrane binding can occur independently of the presence of cholesterol, cholesterol can even delay the cytotoxicity, such as for ginsenoside Rh2, and phospholipids or sphingomyelin play an important role in these interactions [7,18]. Thus, different mechanisms exist, cholesterol-dependent and -independent, that are involved in saponin-induced membrane permeabilization, depending on the structure of saponins [11]. However, recent in vitro experiments and the monolayer simulations of membrane binding of the sea cucumber glycoside frondoside A, confirmed previous findings that suggest the presence of cholesterol is essential to the strong membranolytic activity of saponins. However, the cholesterol-independent, weak binding of the glycoside to the membrane phospholipids, driven by the lipophilic character of the aglycone, was discovered. Then saponins assemble into complexes with membrane cholesterol followed by the accumulation of saponin-sterol complexes into clusters that finally induce curvature stress, resulting in membrane permeabilization and pore formation [7].

The aims of this study were: the analysis of SAR data for a broad series of sea cucumber glycosides, mainly obtained by our research team over recent years on different tumor cell lines and erythrocytes and additionally the explanation for these data by modelling the interactions of the glycosides from the sea cucumber *Eupentacta fraudatrix* with the constituents of model red blood cell membrane through the full-atom molecular dynamics (MD)

simulation. Such an investigation appears even more relevant since different molecules and their complexes composing of cell membranes, for example, cholesterol-enriched lipid rafts, have continued to attract attention as the factors involved in tumorigenesis and a number of cellular pathways related to cell survival, proliferation, and apoptosis [19]. Therefore, it may be of great advantage to modulate the interactions of the membrane constituents by membrane-active compounds, such as triterpene glycosides. An *in silico* technique was applied to reinforce the numerous experimental observations (SAR) by modelling a multitude of inter-molecular interactions at a high spatial (atomic level) and temporal (nanosecond) resolution within a simulation framework that can reconstitute the natural behavior on the basis of physical interactions [20,21]. Such *in silico* MD simulations can be regarded as a “computational microscope” capable of visualizing molecular behavior with unprecedented precision [22].

2. Results and Discussion

2.1. Structure-Activity Relationships (SAR) Observed in the Glycosides from Sea Cucumbers

The triterpene glycosides of sea cucumbers are natural compounds that have been investigated for a long time. Several hundred structures of the glycosides are now known from the representatives of different orders of the class Holothuroidea. The finding of a significant number of new glycosides by our research team, especially over recent years, led to the broadening of the knowledge of their great structural diversity. This facilitated SAR highlighting through the comparative analysis of their structural features, including both carbohydrate chain composition and architecture, aglycone structures, and their bioactivity (cytotoxic and hemolytic action).

It became obvious that glycosides cytotoxic activity depends not only on their structures, but also on the type of processed cells differing by composition and functional peculiarities of their membranes [1]. Analyzing the majority of tested compounds, it has been revealed that the membranes of erythrocytes are more sensitive to the glycoside membranolytic action than the other tested cells such as mouse spleen lymphocytes, ascites of mouse Ehrlich carcinoma, and neuroblastoma Neuro 2a or normal epithelial JB-6 cells. This regularity was observed in the glycosides of the *Actinocucumis typica* [23], *Colochirus robustus* [24], *Massinium magnum* [25,26], *Eupentacta fraudatrix* [27–29], *Psolus fabricii* [30,31], and *Colochirus quadrangularis* [32] sea cucumbers. One of the explanations for this phenomenon may be the enrichment of red blood cell membranes with cholesterol [10].

The structures of holothuroids’ triterpene glycosides vary in a number of structural features while retaining the general plan of molecular structure. The influence of structural signs such as the monosaccharide composition and architecture of carbohydrate chains, the quantity and positions of sulfate groups, the type of aglycone, and the structure of a side chain on the activity of the glycosides is significant.

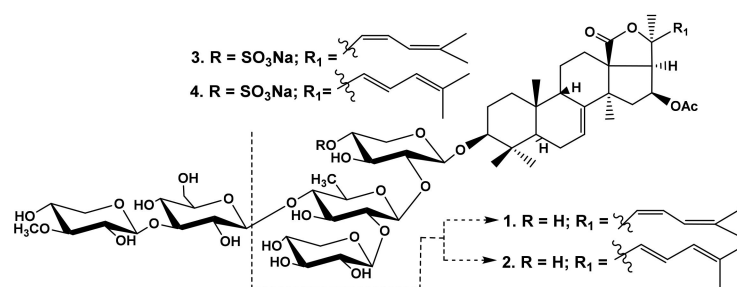
2.1.1. The Dependence of the Glycosides Hemolytic Activity on Their Carbohydrate Chain Structure

It was earlier noticed that the presence of a linear tetrasaccharide chain is necessary for the membranolytic action of the glycosides, that glycosides with quinovose as the second sugar unit in the chain are more active than those with glucose or xylose, and that the sulfate group at C-4 Xyl1 increases the activity of tetraosides and pentaosides with sugar parts branched by C-2 Qui2, however the sulfate groups at C-6 Glc3 and C-6 MeGlc4 of such pentaosides significantly decrease the activity [4,33,34].

In fact, the comparison of the hemolytic activities (Table 1) of cucumariosides B₁ (1) and B₂ (2) from *E. fraudatrix* with a trisaccharide chain with the monosaccharide residues attached to each other by β -(1→2)-glycosidic bonds [35], and the activity of cucumariosides H₅ (3) and H (4) (Figure 1) with pentasaccharide monosulfated chains [36] revealed the significance of the linear tetrasaccharide fragment with terminal *O*-methylated sugar residue, as the compounds 1, 2 were almost not active.

Table 1. The hemolytic activities (synoptic data from the corresponding publications) of the glycosides 1–59 against mouse erythrocytes.

Glycoside	ED ₅₀ , μM/mL	Glycoside	ED ₅₀ , μM/mL	Glycoside	ED ₅₀ , μM/mL
Cucumarioside B ₁ (1)	>100	Psolusoside K (21)	>100	Cucumarioside A ₁₀ (41)	20.00
Cucumarioside B ₂ (2)	18.8	Typicoside B ₁ (22)	0.33	Cucumarioside I ₁ (42)	23.24
Cucumarioside H ₅ (3)	3.2	Typicoside C ₂ (23)	0.18	Cucumarioside I ₄ (43)	75.00
Cucumarioside H (4)	3.8	Cladoloside I ₁ (24)	1.10	Cucumarioside A ₈ (44)	0.70
Magnumoside A ₂ (5)	33.33	Cladoloside I ₂ (25)	2.04	Cucumarioside A ₇ (45)	>100
Magnumoside A ₃ (6)	12.53	Cladoloside J ₁ (26)	1.37	Cucumarioside A ₉ (46)	>100
Magnumoside A ₄ (7)	20.12	Cladoloside K ₁ (27)	0.18	Cucumarioside A ₁₁ (47)	>100
Magnumoside B ₁ (8)	49.57	Cladoloside L ₁ (28)	0.82	Cucumarioside A ₁₄ (48)	>100
Magnumoside B ₂ (9)	58.11	Psolusoside L (29)	2.42	Cucumarioside I ₃ (49)	>100
Magnumoside B ₃ (10)	8.49	Psolusoside M (30)	67.83	Colochiroside B ₁ (50)	39.5
Magnumoside B ₄ (11)	1.42	Psolusoside Q (31)	>100	Typicoside C ₁ (51)	6.25
Magnumoside C ₁ (12)	6.97	Psolusoside P (32)	10.92	Cladoloside D ₂ (52)	10.40
Magnumoside C ₂ (13)	16.20	Quadrangularisoside B ₂ (33)	0.51	Cladoloside K ₂ (53)	11.41
Magnumoside C ₃ (14)	17.80	Quadrangularisoside D ₂ (34)	3.31	Cladoloside D ₁ (54)	0.67
Magnumoside C ₄ (15)	6.52	Quadrangularisoside E (35)	2.04	Quadrangularisoside A (55)	1.57
Psolusoside A (16)	1.4	Colochiroside C (36)	2.5	Quadrangularisoside A ₁ (56)	1.11
Psolusoside E (17)	0.23	Psolusoside F (37)	2.8	Psolusoside D ₃ (57)	1.12
Psolusoside H (18)	2.5	Colochiroside B ₂ (38)	37.02	Psolusoside D ₅ (58)	12.37
Psolusoside H ₁ (19)	2.7	Cucumarioside A ₃₋₂ (39)	40.6	Cucumarioside A ₂ (59)	4.70
Psolusoside J (20)	>100	Cucumarioside A ₁ (40)	0.07		

**Figure 1.** Structures of the glycosides 1–4 from *Eupentacta fraudatrix*.

The analysis of the data on the hemolytic activity of the glycosides from *M. magnum*, with identical aglycones and differing by the oligosaccharide chain structures, demonstrates that the influence of the carbohydrate chain structure indirectly depends on its combination with different aglycones. There were three groups of the glycosides in *M. magnum*: monosulfated biosides (magnumosides of the group A (5–7)), monosulfated tetraosides (magnumosides of the group B (8–11)) and disulfated tetraosides (magnumosides of the group C (12–15)) (Figure 2), all were attached to non-holostane aglycones with 18(16)-lactone differing by the side chain structures [25,26].

In the series of magnumosides B₁ (8) and C₁ (12) and magnumosides A₂ (5), B₂ (9), C₂ (13), with the hydroxyl group in the aglycone side chains, the disulfated tetraosides 12 and 13 were the most active compounds, while in the series of magnumosides A₃ (6), B₃ (10), C₃ (14) and magnumosides A₄ (7), B₄ (11), C₄ (15), which comprised the side chains with a double bond, the monosulfated tetraosides 10 and 11 showed the strongest effect (Table 1). Magnumosides of group A (5–7) demonstrated considerable hemolytic effects despite the absence of a tetrasaccharide linear fragment (Table 1). A compensation for the absence of two sugars by a sulfate at C-4 of the first xylose residue was earlier described for sea cucumber glycosides with 18(20)-lactone in aglycones. [5,33].

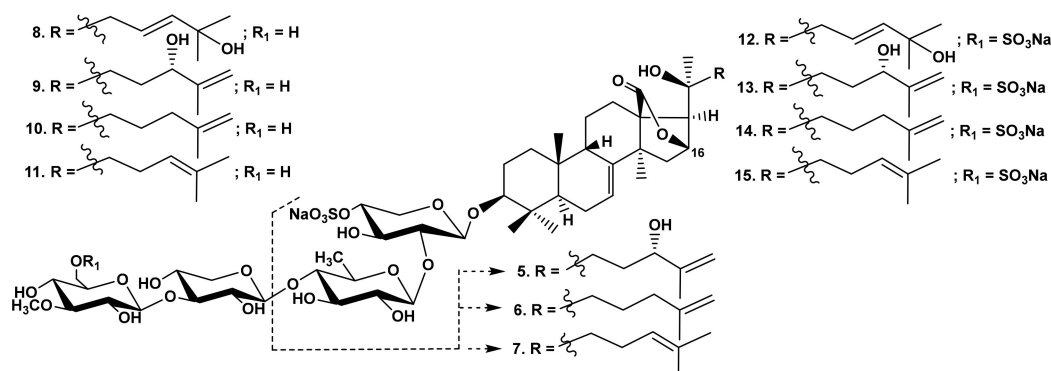


Figure 2. Structures of the glycosides 5–15 from *Massinum magnum*.

The interesting observations were made when the activity of the glycosides from the sea cucumber *Psolus fabricii* (Figure 3) was analyzed [30,31]. Psulososides A (16) and E (17) having linear tetrasaccharide sugar moieties were the strongest cytotoxins in this series, but the activity of psulososides H (18) and H₁ (19) (the glycosides with trisaccharide chains) was close to that of the linear tetraosides 16, 17 (Table 1) despite the absence of tetrasaccharide linear moiety and the change in the second unit (quinovose) in the chain of 16, 17 to glucose residue in 18, 19. However, psulososides J (20) and K (21) with tetrasaccharide chains branched by C-4 Xyl1 and three sulfate groups were completely inactive despite the presence of holostane (i.e., with 18(20)-lactone) aglycones.

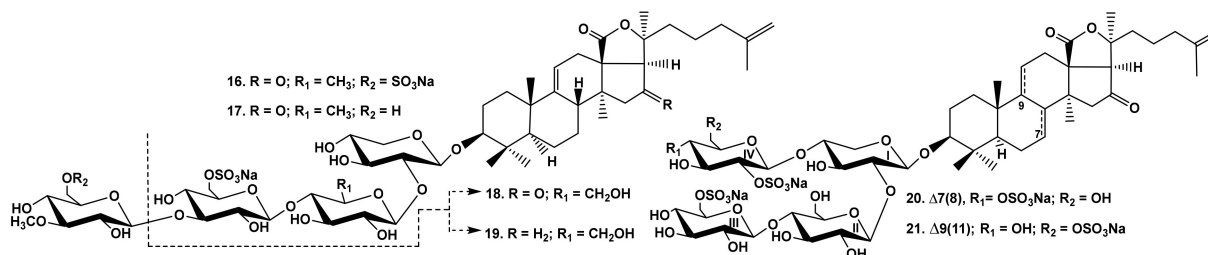


Figure 3. Structures of the glycosides 16–21 from *Psolus fabricii*.

The majority of the glycosides found in the sea cucumber, *Cladolabes schmeltzii*, and characterized by penta- or hexasaccharide moieties branched by C-4 Xyl1, demonstrated strong hemolytic action that was only slightly dependent on their monosaccharide composition. The general trend observed was that hexaosides are more active than pentaosides [37–41].

Therefore, the influence of carbohydrate chain structure on the activity of glycosides is mediated by its combination with the aglycone, however, the general trend is that more developed (tetra-, penta- and hexa-saccharide) sugar moieties provide higher membranolytic action.

2.1.2. The Dependence of Hemolytic Activity of the Glycosides on the Positions and Quantity of Sulfate Groups

The comparison of the hemolytic effects of typicosides B₁ (22) and C₂ (23) from *A. typica* [23] (Figure 4)–linear tetraosides differing by the quantity of sulfate groups showed that the disulfated compound 23 is more active than a monosulfated one (Table 1). High hemolytic activity was demonstrated by the sulfated glycosides from *C. schmeltzii* [39]–cladolosides of groups I (24, 25) and J₁ (26), with pentasaccharide chains branched by C-4 Xyl1 with the sulfate group at C-6 MeGlc in the bottom or upper semi-chains, correspondingly, as well as cladolosides K₁ (27) and L₁ (28)–with monosulfated hexasaccharide chains differing by the sulfate group position (Figure 4). This trend was also confirmed by SAR

demonstrated by the glycosides from *P. fabricii* [31]. Psolusoside L (29) (Figure 5) was strongly hemolytic in spite of the presence of three sulfate groups at C-6 of two glucose and 3-O-methylglucose residues in the pentasaccharide chain branched by C-4 Xyl1. Thus, the presence of sulfate groups attached to C-6 of monosaccharide units did not decrease the activity of pentaosides branched by C-4 Xyl1 in comparison to that of pentaosides branched by C-2 Qui2 [4,33].

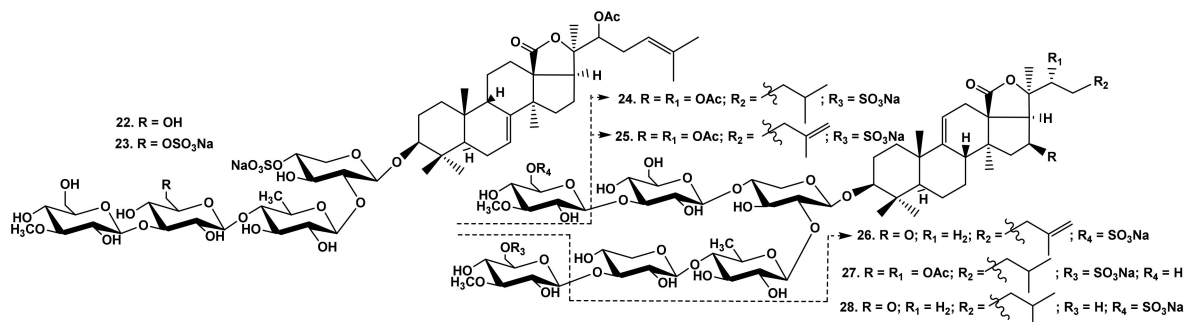


Figure 4. Structures of glycosides 22 and 23 from *Actinocucumis typica* and 24–28 from *Cladolabes shcmeltzii*.

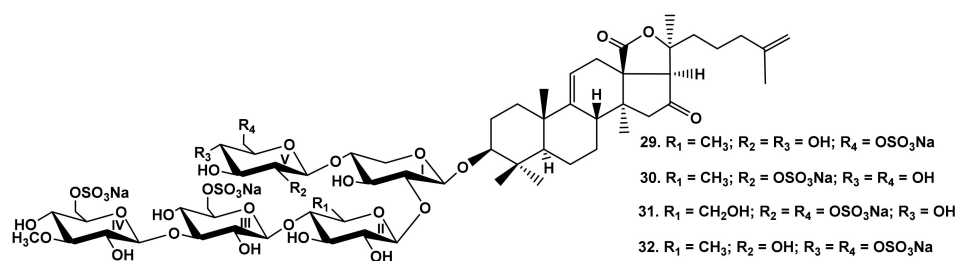


Figure 5. Structures of the glycosides 29–32 from *Psolus fabricii*.

The influence of sulfate position is clearly reflected through the comparison of the activity of psolusosides M (30) and Q (31). The latter glycoside was characterized by the sulfate position attached to C-2 Glc5 (the terminal residue), that caused an extreme decrease in its activity (Table 1). Even the tetrasulfated (by C-6 Glc3, C-6 MeGlc4, C-6 Glc5, and C-4 Glc5) psolusoside P (32) was much more active than trisulfated psolusoside M (30) containing the sulfate group at C-2 Glc5 (Figure 5).

The analysis of SAR in the raw of glycosides from the sea cucumbers *Colochirus quadrangularis* [32] (quadrangularisosides B₂ (33), D₂ (34), and E (35)), *C. robustus* [24] (colochiroside C (36)) (Figure 6) and *P. fabricii* [30] (psolusosides A (16), E (17) (Figure 3), and F (37)) (Figure 6) with the same holostane aglycone and linear tetrasaccharide chains and differing by the third monosaccharide residue and the number and positions of sulfate groups, showed that they all were strong hemolytics (Table 1). However, the presence of a sulfate group at C-4 or C-6 of terminal MeGlc residue resulted in approximately a tenfold decrease in activity, while the sulfation of C-3 Qui2 or C-6 Glc3 did not decrease the hemolytic action.

Hence, the influence of sulfate groups on the membranolytic action of triterpene glycosides depends on the architecture of their carbohydrate chains and the positions of attachment of these functional groups.

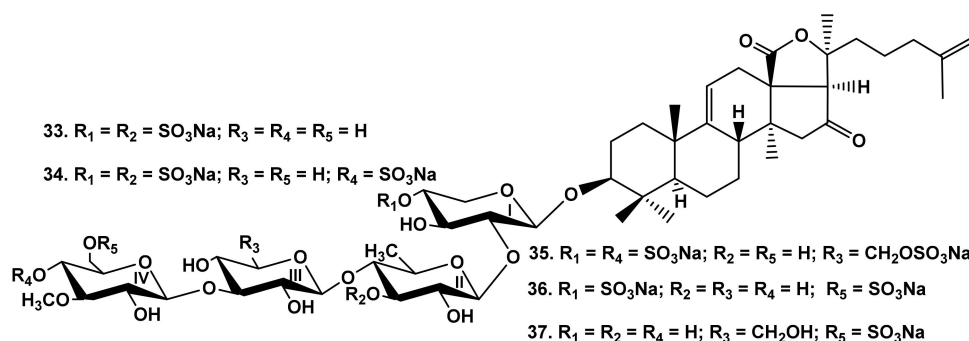


Figure 6. Structures of the glycosides 33–35 from *Colochirus quadrangularis*, 36 from *Colochirus robustus* and 37 from *Psolus fabricii*.

2.1.3. The Dependence of Hemolytic Activity of the Glycosides on Aglycone Structure

In the earlier studies of glycoside SAR, the necessity of the presence of a holostane-type aglycone (with 18(20)-lactone), was noticed for the compound to be active. The glycosides containing non-holostane aglycones (i.e., having 18(16)-lactone, without a lactone with a shortened or normal side chain), as a rule, demonstrate only weak membranolytic action [4,33]. However, different functional groups attached to polycyclic nucleus or the side chain of holostane aglycones can significantly influence the membranotropic activity of the glycosides.

All the glycosides isolated from *M. magnum* contain non-holostane aglycones with 18(16)-lactone, 7(8)-double bond and a normal (non-shortened) side chain. Despite this fact, the compounds demonstrated high or moderate hemolytic effects (Table 1) (except for the compounds containing OH-groups in the side chains) [25,26]. Nevertheless, the comparison of hemolytic activity of the pairs of compounds (Table 1) colochiroside B₂ (38) (Figure 7) and magnumoside B₁ (8), as well as colochiroside C (36) and magnumoside C₃ (14), and differing by the aglycones nuclei (holostane and non-holostane, correspondingly), showed that compounds 36 and 38, which contained the holostane aglycones, were more active, and this is consistent with the earlier conclusions.

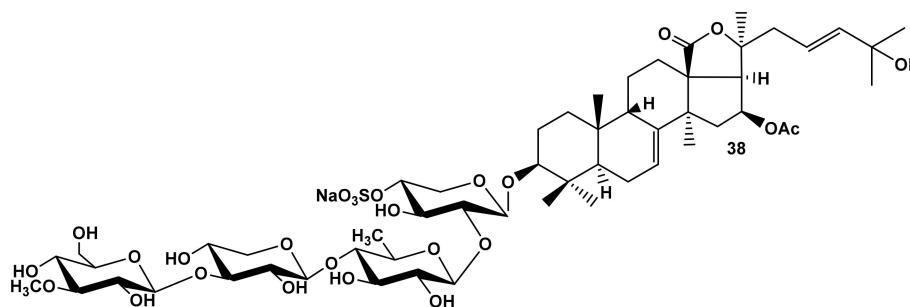


Figure 7. Structure of colochiroside B₂ (38) from *Colochirus robustus*.

Additionally, the glycosides of the sea cucumber, *Cucumaria fallax* [42], did not display any activity due to containing unusual hexa-*nor*-lanostane aglycones with an 8(9)-double bond and without a lactone. The only glycoside from this series, cucumarioside A₃-2 (39) (Figure 8), that was moderately hemolytic (Table 1) was characterized by hexa-*nor*-lanostane aglycone, but, as typical for the glycosides of sea cucumbers, having a 7(8)-double bond and 9 β -H configuration, which demonstrates the significance of these structural elements for the membranotropic action of the glycosides.

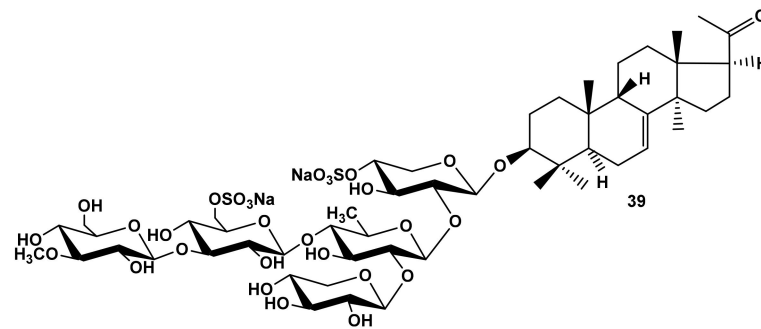


Figure 8. Structure of cucumarioside A₃-2 from *Cucumaria fallax*.

The influence of the side chain length and character of a lactone (18(20)- or 18(16)-) is nicely illustrated by the comparative analysis of the hemolytic activity of the series of glycosides from *E. fraudatrix* (cucumariosides A₁ (40) and A₁₀ (41) [28,29]; cucumariosides I₁ (42) and I₄ (43) [43]) (Figure 9), which indicates that the presence of a normal side chain is essential for the high membranolytic effect of the glycoside.

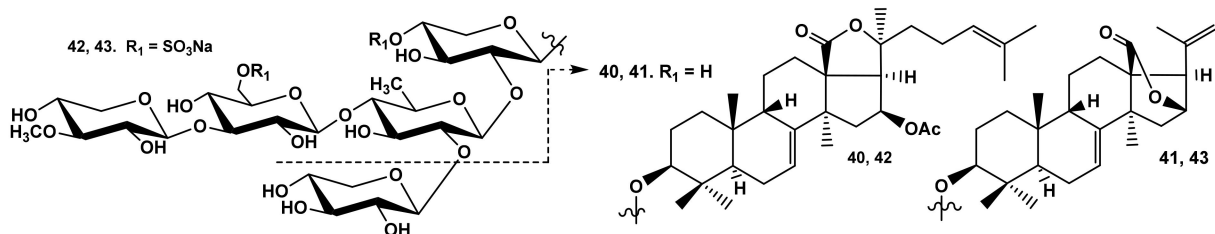


Figure 9. Structures of the glycosides 40–43 from *Eupentacta fraudatrix*.

Unexpectedly high hemolytic activity was displayed by cucumarioside A₈ (44) from *E. fraudatrix* [29] (Figure 10) with unique non-holostane aglycone and without lactone but with hydroxy-groups at C-18 and C-20, which can be considered as a biosynthetic precursor of the holostane aglycones. Its strong membranolytic action (Table 1) could be explained by the formation of an intramolecular hydrogen bond between the atoms of aglycone hydroxyls resulting in the spatial structure of the aglycone becoming similar to that of holostane-type aglycones. Noticeably, it is of special interest to check this issue by *in silico* calculations to clarify the molecular mechanism of membranotropic action of 44.

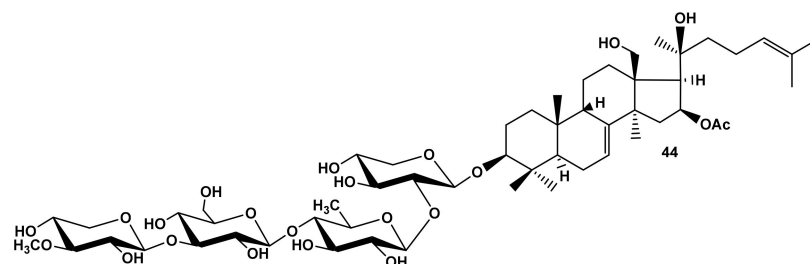


Figure 10. Structure of cucumarioside A₈ (44) from *Eupentacta fraudatrix*.

2.1.4. The Influence of Hydroxyl Groups in the Aglycones Side Chain to Hemolytic Activity of the Glycosides

A strong activity-decreasing effect of the hydroxyl groups in the aglycone side chains was revealed for the first time when the bioactivity of the glycosides from *E. fraudatrix* was studied [27–29,43]. In fact, cucumariosides A₇ (45), A₉ (46), A₁₁ (47), and A₁₄ (48), as well as I₃ (49), were not active against erythrocytes (Table 1) (Figure 11).

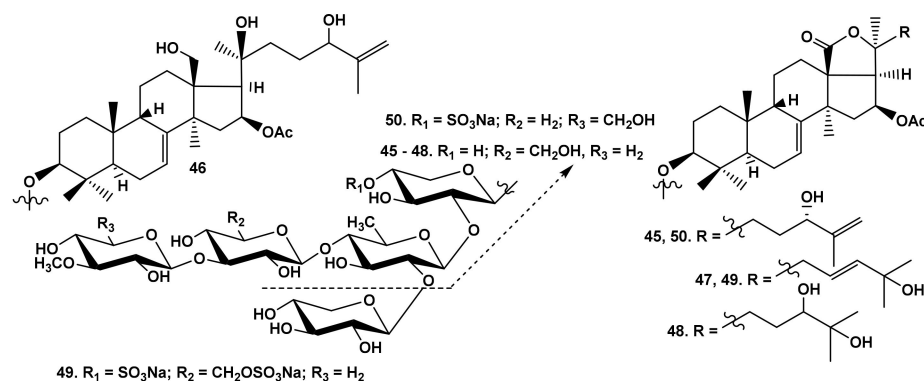


Figure 11. Structures of the glycosides 45–49 from *Eupentacta fraudatrix* and 50 from *Colochirus robustus*.

However, colochirosides B₁ (50) (Figure 11) and B₂ (38) from *C. robustus* [24], with the same aglycones as cucumariosides A₇ (45) and A₁₁ (47), correspondingly, but differing by the third (Xylose) and terminal monosaccharide residues (3-O-MeGlc) and the presence of sulfate group at C-4 Xyl1, demonstrated moderate hemolytic activity (Table 1). The activity of typicoside C₁ (51) from *A. typica* [23] as well as cladolosides D₂ (52) and K₂ (53) from *C. schmeltzii* [40,41], with a 22-OH group in the holostane aglycones, was significantly lower (Table 1) than that of typicoside C₂ (23) and cladolosides D₁ (54) (Figure 12) and K₁ (27), correspondingly, containing a 22-OAc group.

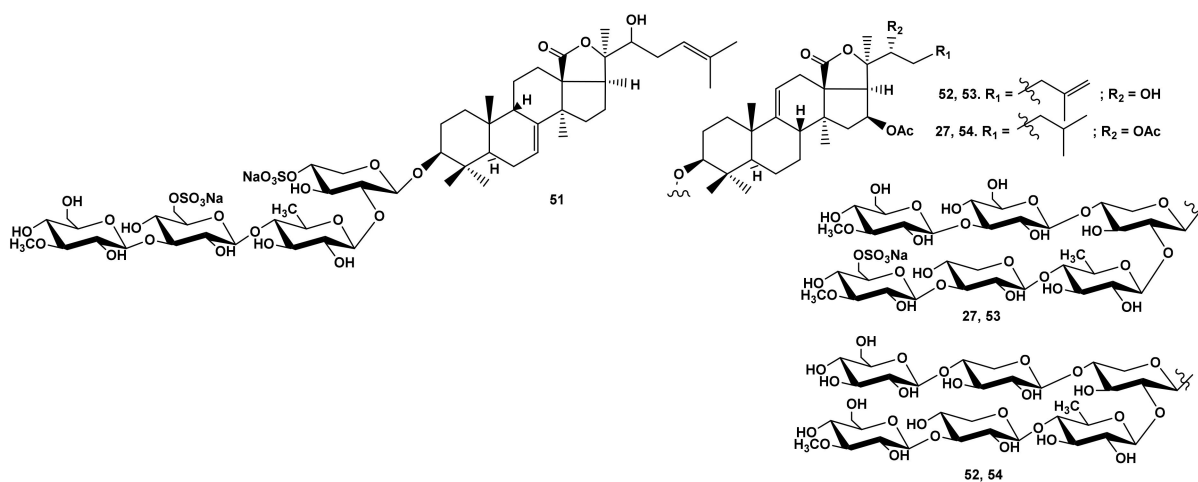


Figure 12. Structures of the glycosides 51–54 from *Cladolabes schmeltzii*.

The same activity-decreasing effect of the hydroxy-group in the side chain was observed for the glycosides of *M. magnum* with non-holostane aglycones (monosulfated glycosides (5, 8, 9)), however, the presence of additional sulfate groups in the carbohydrate chains of 12, 13 compensated this influence to some extent (Table 1).

Recently, the glycosides containing hydroperoxyl groups in the aglycone side chains were found in sea cucumbers *C. quadrangularis* (quadrangularisosides A (55) and A₁ (56) [32]) and *P. fabricii* (psolusoside D₃ (57) [44]) (Figure 13). The comparative analysis of their hemolytic activity with that of their structural analogs that contained hydroxyl groups in the same positions (colochirosides B₂ (38), B₁ (50), and psolusoside D₅ (58), correspondingly) showed that the influence of OOH-functionalities was not so negative (Table 1).

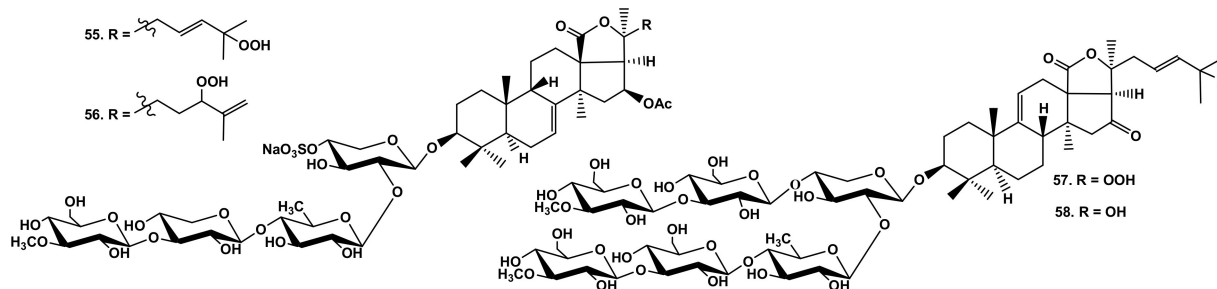


Figure 13. Structures of glycosides 55 and 56 from *Colochirus quadrangularis* and 57 and 58 from *Psolus fabricii*.

2.1.5. Correlation Analysis

To determine the structural elements of glycosides that might be responsible for membrane recognition, a set of physical properties of fifty-nine glycosides (represented in Table 1) were analyzed with MOE 2020.0901 CCG software [45]. Models of the spatial structure of the studied glycosides were built, protonated at pH 7.4, and subjected to energy minimization and a conformational search with MOE 2020.0901 CCG, and the dominant glycoside conformations were selected. The numerical descriptions or characterizations of the molecules that provide their physical properties such as the octanol/water partition coefficient, the polar surface area, the van der Waals (VDW) volume, the approximation to the sum of VDW surface areas of pure hydrogen bond acceptors/donors, the approximation to the sum of VDW surface areas of hydrophobic/polar atoms, etc. (296 in total), as well as their correlation matrix, were calculated with the QuaSAR-Descriptor tool of MOE 2020.0901 CCG software [45] (Figure S1). The correlation analysis did not reveal any strong direct correlation between the hemolytic activities of these compounds *in vitro* (Table 1) and certain calculated molecular 2D and 3D descriptors. Nevertheless, moderate positive correlations of their activity with the atomic contribution of the octanol/water partition coefficient [46], the total negative VDW surface area (\AA^2), the number of oxygen atoms, the atomic valence connectivity index, the kappa shape indexes [47], which describe the different aspects of molecular shape, and the molecular VDW volume (\AA^3) were disclosed. Therefore, an obvious joint effect of the molecular shape and volume (including the carbohydrate moiety shape and volume), the negative charge surface distribution, and the oxygen atom content on the membranotropic properties of the glycosides was observed. These results indicate the extremely complex nature of relationships between the structure of glycosides and their membranolytic action.

The analysis of SAR of the broad series of the glycosides from sea cucumbers also confirms the complicated and ambiguous character of these relationships because the impact in the membranotropic action of a certain structural element depends on the combination of such elements in the glycoside molecule. Nevertheless, there are some structural features causing the activity of the glycosides to be significant:

- The presence of a developed carbohydrate chain composed of four to six monosaccharide residues or a disaccharide chain with a sulfate group;
- The availability of 18(20)- or 18(16)-lactone and a normal (non-shortened) side chain;
- The presence of 9 β -H, 7(8)-ene fragment, or 9(11)-double bond.

The influence of sulfate groups on the membranotropic action of the glycosides depends on the architecture of the sugar chain and the positions of sulfate groups. Hydroxyl groups attached to different positions of aglycone side chains extremely decrease the activity.

2.2. *In Silico* Analysis of the Interaction of the Glycosides from the Sea Cucumber *Eupentacta fraudatrix* with the Model Membrane

The molecular mechanisms of action of membranotropic compounds to the natural cell membranes are difficult to observe directly with any experimental techniques. Moreover,

the lipid composition of membranes of diverse eukaryotic cell types varies to a great extent. The MD simulation providing information at the molecular level has become an increasingly popular “molecular-specific” technique for the study of issues related to bioactive molecule interactions with the membranes due to the rise of computing power, the development of methodologies, software, as well as the force field parameters. Nevertheless, artificial lipid bilayer membranes are suitable models for such investigations providing results consistent with the data obtained in the experiments with different cell lines. In this investigation the lipid composition of model membrane was chosen taking into account the balance between its complexity (resemblance to reality) and the feasibility of biophysical observations to interpret. The model of the symmetrical bilayer membrane containing two or three lipid types (phosphatidylcholine, sphingolipid, and sterol) is the most frequently used. Therefore, the artificial model of the erythrocyte-mimicking membrane constituting of phosphatidylcholine (POPC), cholesterol (CHOL), and palmitoyl-sphingomyelin (PSM) or 1-palmitoyl-2-oleoyl-sn-glycero-3-phosphoethanolamine (POPE) for the outer or inner leaflet, respectively, in a saline solution environment, was constructed based on the lipid composition of red blood cell membranes known to contain approximately 48% CHOL, 28% phosphatidylcholine and 24% sphingomyelin in the outer membrane leaflet, as well as phosphoethanolamine in the inner membrane leaflet [10,48].

To determine the membrane molecular targets of the binding glycosides, the simulations of full-atom molecular dynamic (MD) for the interactions of cucumariosides A₁ (40), A₂ (59), A₈ (44), and A₇ (45) from the sea cucumber *Eupentacta fraudatrix* (Figure 14) (hemolytic activities demonstrated by these compounds in vitro are presented in Table 1), differing from each other by the side chain or aglycone (for 44) structures, with the model membrane for 600 ns time length (for each) were conducted (see Materials and Methods for details). The same MD simulations protocol was applied for the solvated bilayer system without the glycoside exposure, to be used as a control.

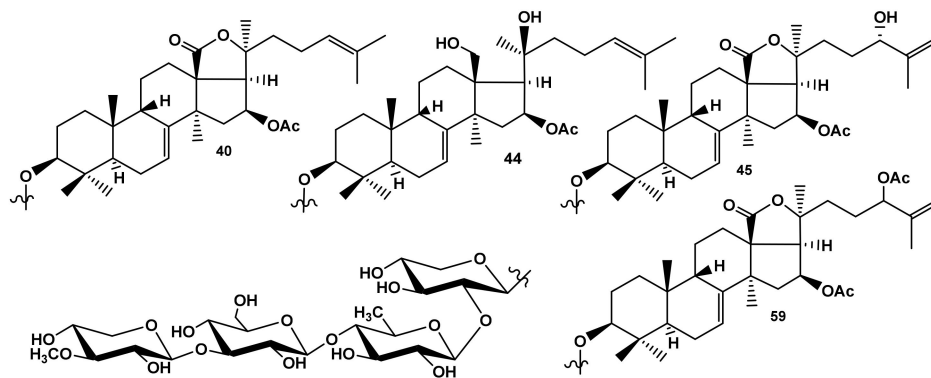


Figure 14. Structure of cucumariosides A₁ (40), A₈ (44), A₇ (45), and A₂ (59) used for in silico analysis of the interaction of the glycosides from the sea cucumber, *Eupentacta fraudatrix*, with the model membrane.

2.2.1. The Modelling of Cucumarioside A₁ (40) Membranotropic Action with MD Simulations

Our results derived from MD simulations of a model membrane system in the presence of cucumarioside A₁ (40) demonstrated that glycoside is able to interact specifically with the PSM of the outer membrane leaflet. The analysis of intermolecular interactions (Figure 15A) of cucumarioside A₁ (40), characterized by 24(25)-double bond, showed the attachment of its carbohydrate chain to membrane sphingomyelin (PSM) by hydrogen bonds (with the energy contribution of -11.94 kcal/M) (Table 2) enabling the anchoring of the glycoside at the interface of the membrane which is similar to dioscin behavior [49].

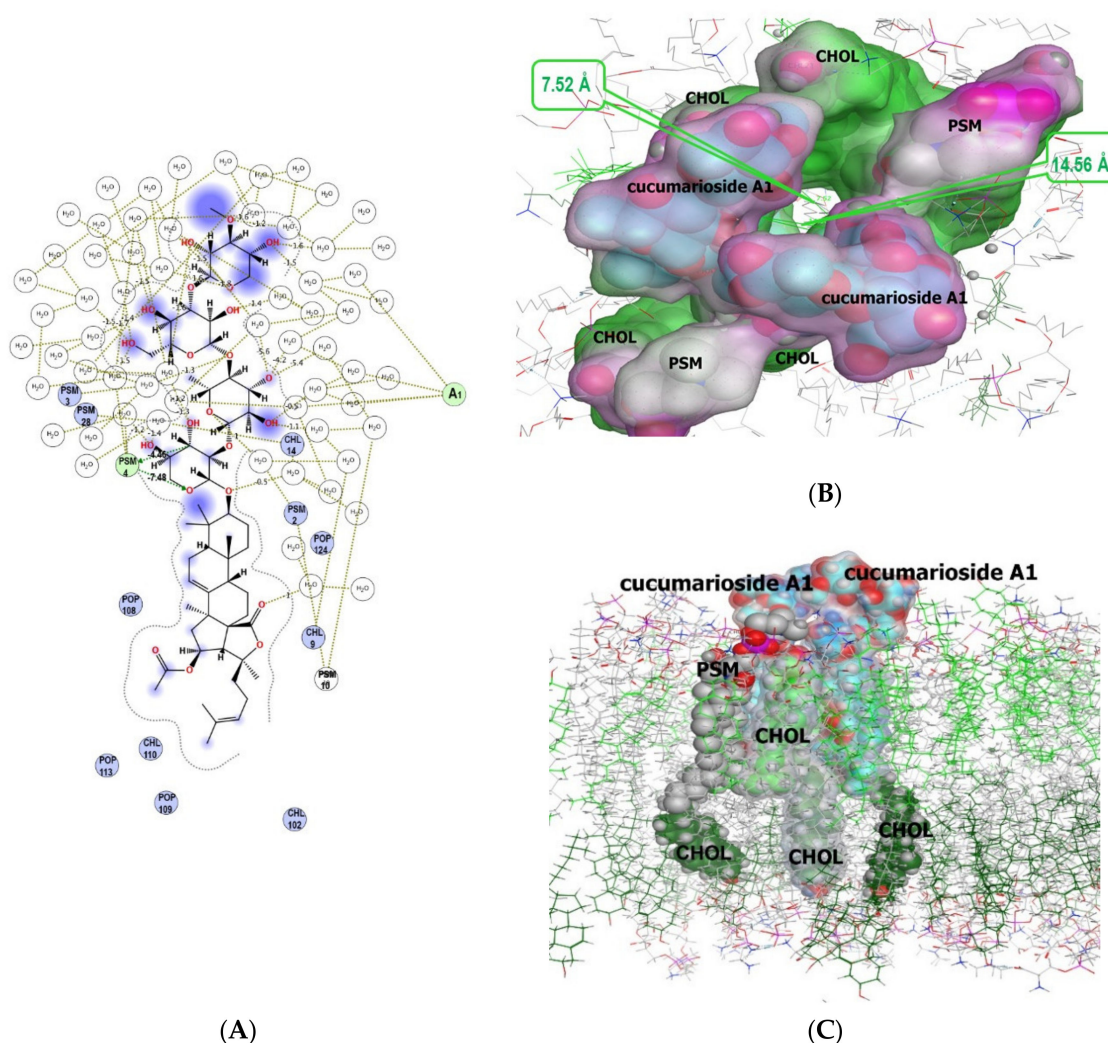


Figure 15. Spatial organization of multimolecular complex formed by two cucumarioside A₁ (40) molecules (I and II) and the model membrane components. **(A)** 2D diagram of noncovalent intermolecular interactions of the glycoside with water-lipid environment. **(B)** Multimolecular complex is presented as a semitransparent molecular surface, colored according to its lipophilicity: hydrophilic areas are pink, lipophilic areas are green, the view is perpendicular to membrane surface. The molecules of solvent and some membrane components are deleted for simplicity. **(C)** Multimolecular complex in membrane environment, the view parallel to membrane surface. The glycoside is presented as cyan “ball” model, POPC+PSM and CHOL molecules (6 Å surrounding glycoside-lipid complex) of outer membrane leaflet are grey and light-green “ball” models, respectively; POPC+PSM and CHOL of inner membrane leaflet, distant from molecular assembly, are presented as grey and dark-green “ball and stick” models, respectively.

Further MD simulations in the system CHOL/POPC/PSM/POPE which was exposed to cucumarioside A₁ (40) molecules demonstrated that glycoside integrates into the outer membrane leaflet leading to an asymmetrical pore formation with 7.52 Å diameter in the central part and 14.56 Å diameter in the entrance (Figure 15B,C). The stoichiometry of the pore forming components, glycoside/CHOL/POPC/PSM, is 2/4/5/6. Hence, cucumarioside A₁ (40) is capable of incorporating into the outer membrane leaflet predominantly through hydrophobic interactions of its aglycone with phospholipids, sphingomyelin, as well as cholesterol, that results in the membrane curvature, followed by its destabilization and permeability changing. It should be noted that during the formation of this multimolecular pore-like structure induced by cucumarioside A₁ (40), sphingomyelin molecules interact tightly with both glycosides and cholesterol through hydrogen-bonding as well as through hydrophobic interactions. Thus, sphingomyelin and cholesterol act as a functional

pair to stabilize these complexes, similar to how they stabilize lipid rafts [22,50]. These data are in accordance with the high hemolytic effect of cucumarioside A₁ (40) (Table 1).

Table 2. Noncovalent intermolecular interactions inside the multimolecular complex formed by two molecules (I and II) of cucumarioside A₁ (40) and components of model lipid bilayer membrane.

Type of Bonding	Cucumarioside A ₁ (40) Molecule	Membrane Component	Energy Contribution, kcal/mol	Distance, Å
Hydrogen bond	I	PSM4	−11.94	4.05
Hydrophobic	I	PSM4	−0.5	3.31
Hydrophobic	I	POPC108	−7.21	3.93
Hydrophobic	I	PSM2	−5.52	4.13
Hydrophobic	I	POP109	−4.69	3.92
Hydrophobic	I	PSM10	−3.71	4.19
Hydrophobic	I	CHOL9	−3.69	4.13
Hydrophobic	I	CHOL14	−2.18	4.01
Hydrophobic	I	POPC124	−1.59	4.02
Hydrophobic	I	POPC113	−0.55	4.13
Hydrophobic	II	CHOL38	−11.05	4.07
Hydrophobic	II	PSM31	−10.82	4.08
Hydrophobic	II	POPC124	−8.38	4.11
Hydrophobic	II	CHOL46	−4.77	4.06
Hydrophobic	II	CHOL14	−4.50	3.93
Hydrophobic	II	PSM28	−1.06	4.15
Hydrophobic	II	PSM74	0.05	3.95

The RMSD value of the heavy atoms of the model membrane phospholipids under cucumarioside A₁ (40) action was 2.89 Å, while for the lipid environment surrounding the glycoside at 10 Å (POPC, CHOL, PSM) it was 4.13 Å. Moreover, the deviation of CHOL heavy atoms in the outer leaflet did not exceed 1.89 Å, while in the inner leaflet the RMSD value was 4.97 Å and reached up to 6.99 Å for some of CHOL molecules (Figure 15C).

2.2.2. The Modelling of Cucumarioside A₈ (44) Membranotropic Action with MD Simulations

The *in silico* study of the action of cucumarioside A₈ (44) from *E. fraudatrix* [29] on a model erythrocyte membrane with MD simulations evidenced that the process apparently occurs in several stages: driven by electrostatic attracting, the glycoside reaches the membrane with its carbohydrate part and can anchor to phospholipid polar heads through hydrogen bonds (Figure 16C and Figure S2), after that its aglycone moiety completely immerses into the lipid layer, and the multimolecular assembly rearranges. Moreover, our computational results have disclosed the feasibility of the glycoside to induce the “pore-like” complex formation inside the membrane with stoichiometry of glycoside/CHOL/POPC/PSM (2/3/2/5) (Figure 16A,B, Table 3). Its assemblage is provided mainly through van der Waals bonds and hydrophobic interactions with PSM and contributes totally to complex formation up to −62.07 kcal/M. Simultaneously, the aglycone of one glycoside molecule (I) is anchored to a PSM head by a hydrogen bond (contributing −1 kcal/M), whereas the carbohydrate moiety of the other molecule (II) stabilizes this complex by another hydrogen bond generated with a POPC molecule (with a contribution of −3.10 kcal/M) (Table 3). This suggests that the mechanism of cucumarioside A₈ (44) hemolytic action is somewhat similar to that of cucumarioside A₁ (40).

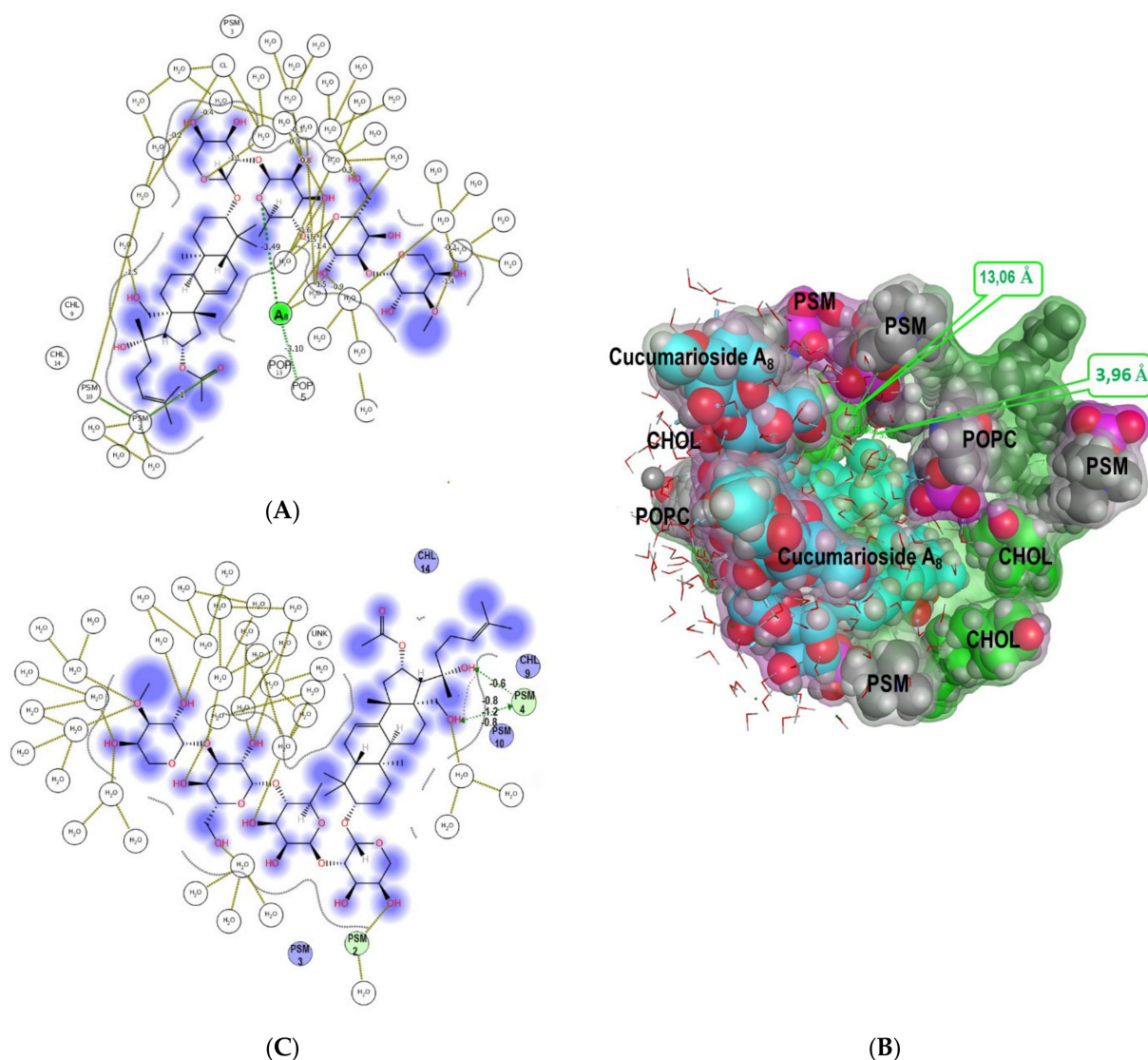


Figure 16. Spatial organization of multimolecular complex formed by two cucumarioside A₈ (44) molecules (I and II) and the model membrane components. (A) 2D diagram of noncovalent intermolecular interactions of the glycoside with water-lipid environment. (B) Multimolecular complex is presented as a semitransparent molecular surface, colored according to its lipophilicity: hydrophilic areas are pink, lipophilic areas are green, the view is perpendicular to membrane surface. The glycoside is presented as cyan “ball” model, POPC+PSM and CHOL molecules (6 Å surrounding glycoside-lipid complex) of the outer membrane leaflet are grey and light-green “ball” models. The molecules of solvent and some membrane components are deleted for simplicity. (C) 2D diagram of noncovalent intermolecular interactions of cucumarioside A₈ (44) with water-lipid environment at the initial stage of glycoside interaction with the model membrane.

The important functional role of hydroxy groups at C-18 and C-20 of cucumarioside A₈ (44) were found to promote an initial stage of glycoside integration into the lipid bilayer by the multiple hydrogen bond formations with sphingomyelin or phosphatidylcholine (Figure 16C). However, the extensive hydrophobic interactions became more energetically favorable at the subsequent stages of the glycoside engagement inside the outer membrane leaflet, allowing it to penetrate rather deeply into the bilayer (Figure S2B). Moreover, further MD simulations have revealed the inner membrane leaflet rearrangement under the influence of cucumarioside A₈ (44). Thus, the aglycone passed through the outer membrane leaflet and initiated the phosphatidylcholine molecule tails to move from the inner layer towards the “pore-like” assembly to generate hydrophobic interactions with

the glycoside side chains (with a contribution of -3.72 kcal/M and -2.02 kcal/M) (Table 3, Figure S2D).

Table 3. Noncovalent intermolecular interactions inside multimolecular complex formed by two molecules (I, II) of cucumarioside A₈ (44) and the components of model lipid bilayer membrane.

Type of Bonding	Cucumarioside A ₈ (44) Molecule	Membrane Component	Energy Contribution, kcal/mol	Distance, Å
Hydrogen bond	II	I	-3.49	3.36
Hydrophobic	II	I	-8.75	3.95
Hydrophobic	II	PSM20	-12.41	4.03
Hydrophobic	I	PSM2	-8.60	4.07
Hydrophobic	II	POPC13	-7.93	3.97
Hydrophobic	II	CHL7	-7.20	4.02
Hydrophobic	II	PSM2	-4.28	4.04
Hydrophobic	I	CHL9	-4.06	4.06
Hydrophobic	I	PSM10	-3.91	4.08
Hydrophobic	II	POPC108 *	-3.72	3.94
Hydrophobic	II	CHL14	-3.23	4.11
Hydrogen bond	II	POPC5	-3.10	2.60
Hydrophobic	I	PSM3	-2.31	3.96
Hydrophobic	II	POPC113 *	-2.02	4.21
Hydrophobic	I	POPC13	-1.39	3.59
Hydrophobic	II	PSM28	-1.01	4.26
Hydrogen bond	I	PSM2	-1.00	3.01

*—the inner membrane leaflet.

The analysis of noncovalent intermolecular interactions in this complex shows that, in contrast to the pore formed by cucumarioside A₁ (40), where the glycoside interacts predominantly with the lipid environment (CHOL/POPC/PSM) of the outer membrane layer (Table 2), the aglycone moieties of cucumarioside A₈ (44) molecules formed rather powerful hydrophobic contacts between each other (with a contribution of -8.75 kcal/M), as well as hydrogen bonds between their carbohydrate parts, contributing approximately -3.49 kcal/M to the complex formation. Apparently, these glycoside/glycoside interactions inside the pore led to a decrease in its diameter to 13.06 Å in the entrance and 3.96 Å in its narrowest part as compared to those for the cucumarioside A₁ (40)-induced pore (Figure 15). This finding suggests that the glycoside 44 is capable of forming pores in the erythrocyte membrane, similar to the glycoside 40, but their size and quantity would be more sensitive to the glycoside concentration. This result is in good agreement with the glycoside activities (Table 1), indicating an order of magnitude higher hemolytic activity of cucumarioside A₁ (40) compared to that of cucumarioside A₈ (44).

2.2.3. The Modelling of Cucumarioside A₂ (59) Membranotropic Action with MD Simulations

MD simulations of interactions of cucumarioside A₂ (59), with a 24-O-acetic group, demonstrated that glycoside bound to both the phospholipids and cholesterol of the outer membrane leaflet causing significant changes in the bilayer architecture and dynamics. The apolar aglycone part of the glycoside and the fatty acid residues of phospholipids interact with each other through hydrophobic bonds (with energy contribution from -1.23 kcal/M to -4.65 kcal/M) and hydrogen bonds (with energy contribution from -0.50 kcal/M to -8.20 kcal/M) (Table 4, Figure 17). The analysis of the energy contributions of different membrane components to the formation of multimolecular complexes including three molecules of cucumarioside A₂ (59) revealed that the glycoside/phospholipid interactions were more favorable compared to the glycoside/cholesterol interactions involving only the aglycone side chain area (Figure 17). One molecule of the glycoside interacted with 3–5 phospholipid molecules involving their polar heads being bound to the polycyclic nucleus and carbohydrate chains while fatty acid tails surrounded the aglycones side chain. Thus, a so-called “phospholipid cluster” is formed around the glycoside causing it

to be partly embedded to the outer leaflet. A rather rigid “cholesterol cluster” is formed under the place of glycoside penetration to the outer membrane leaflet due to the lifting of cholesterol molecules from the inner leaflet attempting, to some extent to substitute the molecules of the outer leaflet which are bound with the glycoside (Figure 17).

Table 4. Noncovalent intermolecular interactions inside multimolecular complex formed by three molecules (I–III) of cucumarioside A₂ (59) and components of model lipid bilayer membrane.

Type of Bonding	Cucumarioside A ₂ (59) Molecule	Membrane Component	Energy Contribution, kcal/mol	Distance, Å
Hydrophobic	I	PSM51	−4.63	4.21
Hydrophobic	I	POPC11	−3.34	3.99
Hydrophobic	I	CHOL92	−0.63	3.89
Hydrophobic	I	POPC49	−1.23	3.99
Hydrogen bond	II	PSM51	−0.49	3.18
Hydrophobic	II	PSM57	−6.19	4.14
Hydrophobic	II	CHOL104	−6.1	3.98
Hydrophobic	II	PSM55	−3.3	4.07
Hydrophobic	II	POPC11	−2.78	4.17
Hydrophobic	II	PSM51	−2.18	4.08
Hydrogen bond	III	POPC49	−8.2	2.49
Hydrophobic	III	POPC11	−3.08	4.20
Hydrophobic	III	POPC49	−1.43	3.91
Hydrophobic	III	CHOL99	−0.67	3.53

Therefore, the agglomerating action of cucumarioside A₂ (59) towards the cholesterol molecules not only in the immediate vicinity of the glycoside but involving the cholesterol molecules from the inner membrane leaflet became clear. However, since cholesterol, with its rather rigid structure, interacts mainly with the aglycone side chain, it continues to be embedded to the outer leaflet, while flexible phospholipid molecules, interacting with both the aglycone and carbohydrate chain, to some extent overlook the outer membrane leaflet. Hence, two so-called “lipid pools” are generated with one of them surrounding carbohydrate and polycyclic moieties of the glycoside and the second one located in the aglycone side chain area (Figure 17B).

Due to the asymmetric distribution of lipids between the membrane monolayers, their properties can differ significantly. POPC and PSM are characterized by saturated fatty acid tails, the asymmetry of leaflets is enhanced by different polar head properties of POPC, PSM, and POPE. Moreover, the presence of CHOL molecules in the bilayer, the content of which is close to 50% in the erythrocyte biomembrane, promotes the “elongation” and alignment of fatty tails of phospholipids parallel to the flat core of CHOL [51]. Our MD simulation results suggest that cucumarioside A₂ (59) apparently induced the disruption of tight CHOL/lipid and lipid/lipid interactions through an extensive hydrophobic area formation in the glycoside’s immediate environment (Figure 17, Table 4). Additionally, the glycoside can provoke the process of CHOL release from the inner monolayer and its accumulation between monolayers or insertion to the outer one, because, unlike POPC, PSM and POPE, which have rather bulk polar heads, the small polar OH-group of CHOL is known to facilitate CHOL relocation between monolayers due to the low energy barrier of the “flip-flop” mechanism [51]. All these properties and forces led to the accumulation of CHOL molecules surround the glycoside, which resulted in an increase in layer viscosity. Simultaneously the CHOL outflow made the inner leaflet more fluid and unbalanced compared to the structured outer one that can cause the generation of non-bilayer disordered membrane architecture. These circumstances cause the inner membrane leaflet to be reorganized followed by the changing of the membrane barrier properties providing the hemolytic action of the glycoside.

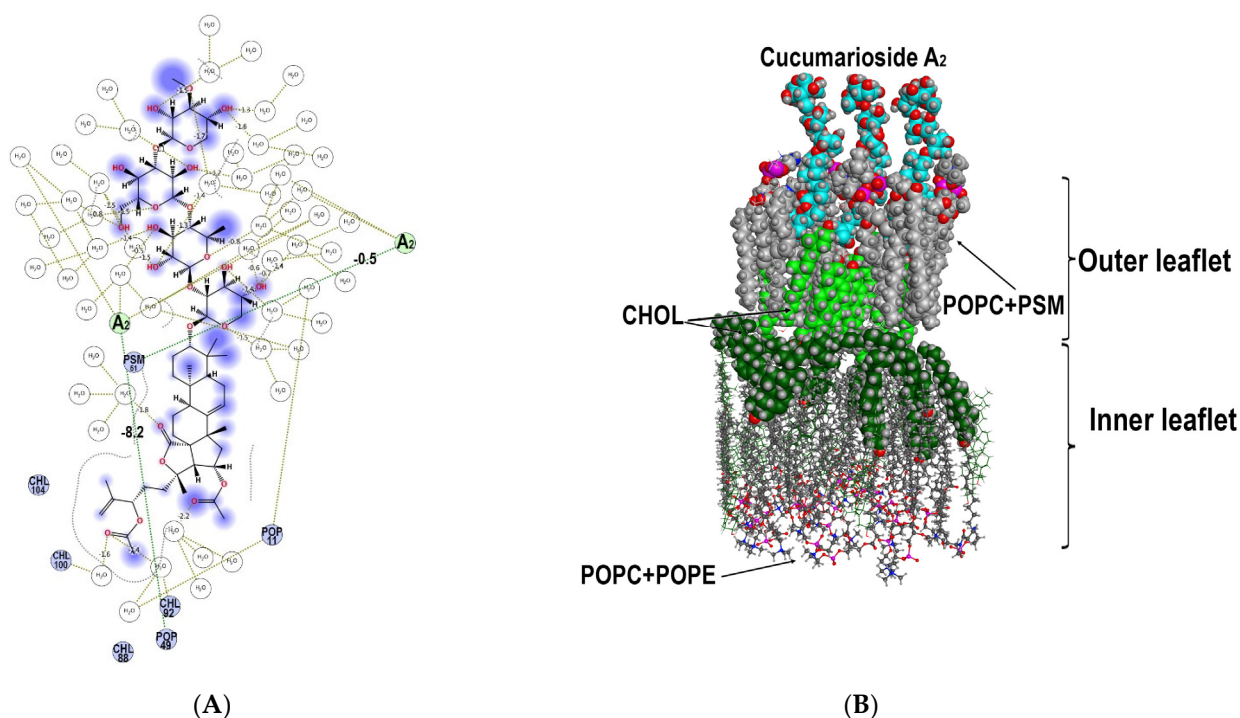


Figure 17. Spatial organization of multimolecular complex formed by three molecules (I–III) of cucumarioside A₂ (59) and the components of model membrane. **(A)** 2D diagram of intermolecular noncovalent interactions of three cucumarioside A₂ (59) molecules and the components of model water/lipid bilayer environment. Hydrogen bonds are green dotted lines. **(B)** Front view to the cucumarioside A₂ (59) multimolecular complex with a model membrane. The glycoside is presented as cyan “ball” model, POPC+PSM and CHOL (6 Å surrounding glycoside) of the outer membrane leaflet are presented as grey and light-green “ball” models, respectively; POPC+POPE and CHOL of inner membrane leaflet, distant from multimolecular assembly, are presented as grey and dark-green “ball and stick” models, respectively; CHOL molecules of the inner membrane leaflet at 5 Å distant from multimolecular complex are presented as a dark-green “ball” model. The molecules of solvent and some membrane components are deleted for simplicity.

Thus, according to our MD simulations, cucumarioside A₂ (59) exposure caused significant change in the architecture of the model membrane bilayer (Figure 17). It should be noted that although the dynamic behavior of the lipid environment of cucumarioside A₁ (40) and cucumarioside A₂ (59) was similar, there were a number of considerable differences. Despite the low RMSD value for all heavy atoms of membrane lipids (3.74 Å), which reflects the mobility of membrane components, the dynamic behavior of those located in the immediate environment of the glycoside molecules was changed to a great extent. So, their RMSD value (10 Å surrounding the glycoside) was 7.47 Å, and for some CHOL molecules, predominantly those forming the inner membrane leaflet, this value reached 17.68 Å.

2.2.4. The Modelling of Cucumarioside A₇ (45) Membranotropic Action with MD Simulations

Cucumarioside A₇ (45) differs from the compounds 40, 44, and 59 by the presence of an OH-group in the aglycone side chain that causes the extremal decreasing in its membranotropic activity (Table 1). In fact, *in silico* simulations of its interactions with model membrane demonstrated only slight interactions with phospholipid polar heads and the absence of glycoside/cholesterol interactions.

Moreover, MD simulations of cucumarioside A₇ (45) interactions showed RMSD values with neighboring lipids was comparable to those observed during MD simulations in the control membrane system and for both did not exceed 2.34 Å. This result indicated no significant changes in lipid packaging induced by cucumarioside A₇ (45); this is in good accordance with hemolytic activity, SAR data (Table 1), as well as other MD simulations which indicated the involvement of the aglycones side chain in the hydrophobic interactions

with phospholipid fatty acid tails and cholesterol. It is obviously that hydroxyl groups in the side chain of **45** impeded such interactions.

3. Materials and Methods

3.1. Model System for Artificial Plasma Membrane Mimicking the Erythrocyte Membrane

An asymmetric model bilayer comprising POPC (1-palmitoyl-2-oleoyl-sn-glycero-3-phosphocholine), CHOL (cholesterol), PSM (palmitoylshingomyeline for outer leaflet), or POPE (1-palmitoyl-2-oleoyl-sn-glycero-3-phosphoethanolamine) for the inner leaflet, respectively, in the ratio 1:2:1 was constructed by remote web resource CHARMM-GUIHMMM Builder [52,53], solvated, and equilibrated during 400 ns for optimal bilayer package.

3.2. Full Atom MD Simulations

Since we did not have any information on the possible orientation of glycosides during their interaction with the membrane, glycoside molecules were added to the previously equilibrated model membrane system and placed at a distance of 11 Å above the outer membrane leaflet. The orientation of the molecules was chosen arbitrarily provided that their long axis was located along the membrane surface (Figure S2A). The model membrane simulation system with the glycosides was resolvated with water (25 Å above and below the membrane) and neutralized with counterions for a simulating box of $200 \times 200 \times 90$ Å, protonated at pH 7.4, and the total potential energy of the systems was minimized with the energy gradient of $0.01 \text{ kcal/mol/Å}^{-1}$ to remove initial unfavorable contacts, then heated from 0 to 300 K for 100 ns and equilibrated at 300 K for another 200 ns.

The MD simulations of the free model membrane system or under the impact of glycosides in water environment were conducted with an Amber 14EHT force field. This was carried out with a checkpoint at 500 ps, a sample time of 10 ps, with Nosé-Poincaré-Andersen Hamiltonian equations of motion (NPA), and a time step of 0.001 ps, at a constant pressure (1 atm) and temperature (300 K) giving a total simulation time of 600 ns using MOE 2020.0901 CCG software [45]. Solvent molecules were treated as rigid. Computer simulations and theoretical studies were performed using cluster CCU "Far Eastern computing resource" FEB RAS (Vladivostok).

MD simulations of the control membrane system demonstrated RMSD value no higher than 2.34 Å.

The analysis of intramolecular interactions as well as the estimation of the interaction energy contribution was made with a ligand interaction suite from MOE 2020.0901 CCG software [45].

3.3. Triterpene Glycosides Chosen for MD Simulations

Cucumarioside A₁ (**40**): $3\beta\text{-O-[3-O-methyl-}\beta\text{-D-xylopyranosyl-(1}\rightarrow\text{3)-}\beta\text{-D-glucopyranosyl-(1}\rightarrow\text{4)-}\beta\text{-D-quinovopyranosyl-(1}\rightarrow\text{2)-}\beta\text{-D-xylopyranosyl]-16}\beta\text{-acetoxyholosta-7,24-diene}$; mp 190 °C; $[\alpha]_{\text{D}}^{20} -15^\circ$ (c 0.1, C₅H₅N).

Cucumarioside A₂ (**59**): $3\beta\text{-O-[3-O-methyl-}\beta\text{-D-xylopyranosyl-(1}\rightarrow\text{3)-}\beta\text{-D-glucopyranosyl-(1}\rightarrow\text{4)-}\beta\text{-D-quinovopyranosyl-(1}\rightarrow\text{2)-}\beta\text{-D-xylopyranosyl]-16}\beta,24\text{-diacetoxyholosta-7,25-diene}$; mp 167 °C; $[\alpha]_{\text{D}}^{20} -17$ (c 0.1, C₅H₅N). HR ESI MS (+) *m/z*: 1179.5555 (calc 1179.5558) [M + Na]⁺.

Cucumarioside A₇ (**45**) is $3\beta\text{-O-[3-O-methyl-}\beta\text{-D-xylopyranosyl-(1}\rightarrow\text{3)-}\beta\text{-D-glucopyranosyl-(1}\rightarrow\text{4)-}\beta\text{-D-quinovopyranosyl-(1}\rightarrow\text{2)-}\beta\text{-D-xylopyranosyl]-16}\beta\text{-acetoxyholosta-24S-hydroxy-7,25-diene}$; mp 183–185 °C; $[\alpha]_{\text{D}}^{20} -5$ (c 0.1, C₅H₅N). HR ESI MS (+) *m/z*: 1137.5460 (calc 1137.5452) [M + Na]⁺.

Cucumarioside A₈ (**44**) $3\beta\text{-O-[3-O-methyl-}\beta\text{-D-xylopyranosyl-(1}\rightarrow\text{3)-}\beta\text{-D-glucopyranosyl-(1}\rightarrow\text{4)-}\beta\text{-D-quinovopyranosyl-(1}\rightarrow\text{2)-}\beta\text{-D-xylopyranosyl]-16}\beta\text{-acetoxy-9}\beta\text{-H-lanosta-7,24-diene-18,20}\beta\text{-diol}$. mp 238–240 °C, $[\alpha]_{\text{D}}^{20} -3$ (c 0.1, C₅H₅N), HR MALDI TOF MS (+) *m/z*: 1125.5812 (calc 1125.5816) [M + Na]⁺.

4. Conclusions

The SAR for the sea cucumber triterpene glycosides illustrated by their action on mouse erythrocytes, is very complicated. Nevertheless, in our study, several clear trends were found, providing significant membranolytic activity for the glycosides, namely: the presence of a developed carbohydrate chain composed of four to six monosaccharide residues (with linear tetrasaccharide fragment) or a disaccharide chain with a sulfate group; the availability of 18(20)- or 18(16)-lactone and a normal (non-shortened) side chain; the presence of 9 β -H, 7(8)-ene fragment or 9(11)-double bond. It was also observed that the influence of sulfate groups on the membranotropic action of the glycosides depends on the architecture of the sugar chain and the positions of sulfate groups. Hydroxyl groups attached to different positions of aglycone side chains extremely decrease the activity.

Using an *in silico* approach of full-atom MD simulations for the investigation of interactions of sea cucumber triterpene glycosides with the molecules composing the model lipid bilayer membrane has resulted in the clarification of several characteristics of the molecular mechanisms of membranolytic action of these compounds. It was revealed that the studied glycosides bound to the membrane surface mainly by hydrophobic interactions and hydrogen bonds, but the mode of such interactions depended on the aglycone side chain structure and varied to a great extent. The formation of multimolecular lipid/glycoside complexes led to membrane curvature followed by the subsequent membranolytic effects of the glycosides. Different mechanisms of glycoside/membrane interactions were discovered for cucumariosides A₁ (40), A₈ (44), and A₂ (59). The first mechanism, inherent for 40 and 44, was realized through the pore's formation differed by the shape, stoichiometry, and the impact of diverse noncovalent interactions into complex assembling, depending on the glycoside structural peculiarities. The second mode of membranotropic action was realized by 59 through the formation of phospholipid and cholesterol clusters in the outer and inner membrane leaflets, correspondingly.

The observed peculiarities of membranotropic action are in good agreement with the corresponding data of *in vitro* hemolytic activity of the investigated compounds [28,29]. In fact, the hemolytic activity of pore-forming cucumariosides A₁ (40) and A₈ (44) were 0.07 and 0.70 $\mu\text{M}/\text{mL}$, correspondingly. The value for cluster-forming cucumarioside A₂ (59) was 4.70 $\mu\text{M}/\text{mL}$, and cucumarioside A₇ (45) demonstrating the weakest capacity to embed the membrane, was not active to the maximal studied concentration of 100.0 $\mu\text{M}/\text{mL}$.

Further *in silico* studies of the relationships of the membrane lipid composition and structural peculiarities of the glycosides demonstrating membranolytic activity are necessary to ascertain the molecular targets of glycoside/membrane bonding and to deepen the understanding of these complex multistage mechanisms.

Supplementary Materials: The following are available online at <https://www.mdpi.com/article/10.3390/md19110604/s1>. Figure S1: The Correlation matrix of the hemolytic activities of glycosides *in vitro* (ED₅₀, $\mu\text{M}/\text{mL}$, Table 1) and certain calculated molecular 2D and 3D descriptors conducted with the QuaSAR-Descriptor tool of MOE 2020.0901 CCG software [45]. Moderate positive correlation of their activity with the atomic contribution to Log of the octanol/water partition coefficient (h_{logP}) [46], the total negative VDW surface area (\AA^2), the number of oxygen atoms (a_{no}), the atomic valence connectivity index (χ_{0v}), kappa shape indexes (Kier) [47], describing different aspects of molecular shape, the molecular VDW volume (Vol, vdw_vol , VSA_acc , (\AA^3)) were disclosed. Figure S2: (A) Initial conformation of cucumarioside A₈ (44) for MD simulations, where the A₈ (44) molecules are placed at a distance of 11 \AA above the outer membrane leaflet with their long axis is directed along the membrane surface. (B) The snapshot of 85 ns MD simulations indicating the cucumarioside A₈ carbohydrate parts come up to the phospholipid heads of the outer membrane leaflet. (C) The snapshot of 130 ns MD simulations indicating the cucumarioside A₈ aglycone pass through the outer membrane leaflet. (D) The last snapshot of MD simulations indicating the aglycone moieties of two cucumarioside A₈ molecules induce the "pore-like" complex formation inside the membrane. The glycoside is presented as cyan "ball" model, POPC+PSM +CHOL are presented as grey stick models. The solvent molecules and some membrane components are deleted for simplicity.

Author Contributions: Conceptualization, A.S.S., V.I.K., and S.A.A.; methodology, E.A.Z.; investigation, A.S.S., E.A.Z., and S.A.A.; writing—original draft preparation, A.S.S., E.A.Z.; writing—review and editing, A.S.S., V.I.K. All authors have read and agreed to the published version of the manuscript.

Funding: Grant from the Russian Foundation for Basic Research No. 19-04-000-14.

Institutional Review Board Statement: Not applicable.

Informed Consent Statement: Not applicable.

Data Availability Statement: Not applicable.

Acknowledgments: The study was carried out with the equipment of the Collective Facilities Center “The Far Eastern Center for Structural Molecular Research (NMR/MS) PIBOC FEB RAS”.

Conflicts of Interest: The authors declare no conflict of interest.

References

1. Aminin, D.L.; Menchinskaya, E.S.; Pislugin, E.A.; Silchenko, A.S.; Avilov, S.A.; Kalinin, V.I. Sea cucumber triterpene glycosides as anticancer agents. In *Studies in Natural Product Chemistry*; Atta-ur-Rahman, Ed.; Elsevier B.V.: Amsterdam, The Netherlands, 2016; Volume 49, pp. 55–105.
2. Kalinin, V.I.; Prokofieva, N.G.; Likhatskaya, G.N.; Schentsova, E.B.; Agafonova, I.G.; Avilov, S.A.; Drozdova, O.A. Hemolytic activities of triterpene glycosides from the holothurian order Dendrochirotida: Some trends in the evolution of this group of toxins. *Toxicon* **1996**, *34*, 475–483. [[CrossRef](#)]
3. Careaga, V.P.; Maier, M.S. Cytotoxic triterpene glycosides from sea cucumbers. In *Handbook of Anticancer Drugs from Marine Origin*; Kim, S.-K., Ed.; Springer International Publishing: Cham, Switzerland, 2015; pp. 515–528.
4. Kalinin, V.I.; Aminin, D.L.; Avilov, S.A.; Silchenko, A.S.; Stonik, V.A. Triterpene glycosides from sea cucumbers (Holothuroidea, Echinodermata), biological activities and functions. In *Studies in Natural Product Chemistry (Bioactive Natural Products)*; Atta-ur-Rahman, Ed.; Elsevier Science Publisher: Amsterdam, The Netherlands, 2008; Volume 35, pp. 135–196.
5. Kalinin, V.I. System-theoretical (holistic) approach to the modelling of structural-functional relationships of Biomolecules and their evolution: An example of triterpene glycosides from sea cucumbers (Echinodermata, Holothuroidea). *J. Theor. Biol.* **2000**, *206*, 151–168. [[CrossRef](#)]
6. Park, J.-I.; Bae, H.-R.; Kim, C.G.; Stonik, V.A.; Kwak, J.Y. Relationships between chemical structures and functions of triterpene glycosides isolated from sea cucumbers. *Front. Chem.* **2014**, *2*, 77. [[CrossRef](#)]
7. Claereboudt, E.J.S.; Eeckhaut, I.; Lins, L.; Deleu, M. How different sterols contribute to saponin tolerant plasma membranes in sea cucumbers. *Sci. Rep.* **2018**, *8*, 10845. [[CrossRef](#)] [[PubMed](#)]
8. Likhatskaya, G.N.; Yarovaya, T.P.; Rudnev, V.V.; Popov, A.M.; Anisimov, M.M.; Rovin, Y.G. Formation of complex of triterpene glycoside of holothurine A with cholesterol in liposomal membranes. *Biofizika* **1985**, *30*, 358–359.
9. Popov, A.M. A Comparative study of the hemolytic and cytotoxic activities of triterpenoids isolated from ginseng and sea cucumbers. *Biol. Bull.* **2002**, *29*, 120–128. [[CrossRef](#)]
10. Deleu, M.; Crowet, J.M.; Nasir, M.N.; Lins, L. Complementary biophysical tools to investigate lipid specificity in the interaction between bioactive molecules and the plasma membrane: A review. *Biochim. Biophys. Acta* **2014**, *1838*, 3171–3190. [[CrossRef](#)] [[PubMed](#)]
11. Lorent, J.H.; Quetin-Leclercq, J.; Mingeot-Leclercq, M.-P. The amphiphilic nature of saponins and their effects on artificial and biological membranes and potential consequences for red blood and cancer cells. *Org. Biomol. Chem.* **2014**, *12*, 8803–8822. [[CrossRef](#)] [[PubMed](#)]
12. Malyarenko, T.V.; Kicha, A.A.; Kalinovsky, A.I.; Dmitrenok, P.S.; Malyarenko, O.S.; Kuzmich, A.S.; Stonik, V.A.; Ivanchina, N.V. New triterpene glycosides from the Far Eastern starfish *Solaster pacificus* and their biological activity. *Biomolecules* **2021**, *11*, 427. [[CrossRef](#)]
13. Aminin, D.; Pislugin, E.; Astashev, M.; Es'kov, A.; Kozhemyako, V.; Avilov, S.; Zelepuga, E.; Yurchenko, E.; Kaluzhskiy, L.; Kozlovskaya, E.; et al. Glycosides from edible sea cucumbers stimulate macrophages via purinergic receptors. *Sci. Rep.* **2016**, *6*, 39683. [[CrossRef](#)]
14. Kersten, G.F.; Crommelin, D.J. Liposomes and ISCOMS as vaccine formulations. *Biochim. Biophys. Acta.* **1995**, *1241*, 117–138. [[CrossRef](#)]
15. Mazeyka, A.N.; Popov, A.M.; Kalinin, V.I.; Avilov, S.A.; Silchenko, A.S.; Kostetsky, E.Y. Complexation between triterpene glycosides of holothurians and cholesterol is the basis of lipid-saponin carriers of subunit protein antigens. *Biophysics* **2008**, *53*, 826–835.
16. Stonik, V.A.; Aminin, D.L.; Boguslavski, V.M.; Avilov, S.A.; Agafonova, I.G.; Silchenko, A.S.; Ponomarenko, L.P.; Prokofieva, N.G.; Chaikina, E.L. Immunostimulatory means Cumaside and pharmaceutical composition on its base. Patent of the Russian Federation No. 2271820, 20 March 2005. Appl. No. 2004120434/17, 2 July 2004.
17. Aminin, D.L.; Chaykina, E.L.; Agafonova, I.G.; Avilov, S.A.; Kalinin, V.I.; Stonik, V.A. Antitumor activity of the immunomodulatory lead Cumaside. *Intern. Immunopharm.* **2010**, *10*, 648–654. [[CrossRef](#)] [[PubMed](#)]

18. Verstraeten, S.L.; Deleu, M.; Janikowska-Sagan, M.; Claereboudt, E.J.S.; Lins, L.; Tyteca, D.; Mingeot-Leclercq1, M.P. The activity of the saponin ginsenoside Rh2 is enhanced by the interaction with membrane sphingomyelin but depressed by cholesterol. *Sci. Rep.* **2019**, *9*, 7285. [[CrossRef](#)] [[PubMed](#)]
19. Mollinedo, F.; Gajate, C. Lipid rafts as major platforms for signaling regulation in cancer. *Adv Biol Regul.* **2015**, *57*, 130–146. [[CrossRef](#)] [[PubMed](#)]
20. Guariento, S.; Bruno, O.; Fossa, P.; Cichero, E. New insights into PDE4B inhibitor selectivity: CoMFA analyses and molecular docking studies. *Mol. Divers.* **2016**, *20*, 77–92. [[CrossRef](#)]
21. Rusnati, M.; Sala, D.; Orro, A.; Bugatti, A.; Trombetti, G.; Cichero, E.; Urbinati, C.; Di Somma, M.; Millo, E.; Galiotta, L.J.V.; et al. Speeding Up the Identification of Cystic Fibrosis Transmembrane Conductance Regulator-Targeted Drugs: An Approach Based on Bioinformatics Strategies and Surface Plasmon Resonance. *Molecules* **2018**, *23*, 120. [[CrossRef](#)]
22. Sezgin, E.; Levental, I.; Mayor, S.; Eggeling, C. The mystery of membrane organization: Composition, regulation and roles of lipid rafts. *Nat. Rev. Mol. Cell Biol.* **2017**, *18*, 361–374. [[CrossRef](#)]
23. Silchenko, A.S.; Kalinovskiy, A.I.; Avilov, S.A.; Andryjaschenko, P.V.; Dmitrenok, P.S.; Martyyas, E.A.; Kalinin, V.I.; Jayasandhya, P.; Rajan, G.C.; Padmakumar, K.P. Structures and biological activities of triterpenoid glycosides A₁, A₂, B₁, C₁ and C₂, triterpene glycosides from the sea cucumbers *Actinocucumis typica*. *Nat. Prod. Commun.* **2013**, *8*, 301–310.
24. Silchenko, A.S.; Kalinovskiy, A.I.; Avilov, S.A.; Andryjaschenko, P.V.; Dmitrenok, P.S.; Kalinin, V.I.; Yurchenko, E.V.; Dolmatov, I.Y. Colochirosides B₁, B₂, B₃ and C, novel sulfated triterpene glycosides from the sea cucumber *Colochirus robustus* (Cucumariidae, Dendrochirotida). *Nat. Prod. Commun.* **2015**, *10*, 1687–1694. [[CrossRef](#)]
25. Silchenko, A.S.; Kalinovskiy, A.I.; Avilov, S.A.; Kalinin, V.I.; Andrijaschenko, P.V.; Dmitrenok, P.S.; Chingizova, E.A.; Ermakova, S.P.; Malyarenko, O.S.; Dautova, T.N. Nine new triterpene glycosides, magnumosides A₁–A₄, B₁, B₂, C₁, C₂ and C₄, from the Vietnamese sea cucumber *Neothyronidium (=Massinum) magnum*: Structures and activities against tumor cells independently and in synergy with radioactive irradiation. *Mar. Drugs* **2017**, *15*, 256. [[CrossRef](#)]
26. Silchenko, A.S.; Kalinovskiy, A.I.; Avilov, S.A.; Kalinin, V.I.; Andrijaschenko, P.V.; Dmitrenok, P.S.; Chingizova, E.A.; Ermakova, S.P.; Malyarenko, O.S.; Dautova, T.N. Magnumosides B₃, B₄ and C₃, mono- and disulfated triterpene tetraosides from the Vietnamese sea cucumber *Neothyronidium (=Massinum) magnum*. *Nat. Prod. Commun.* **2017**, *12*, 1577–1582.
27. Silchenko, A.S.; Kalinovskiy, A.I.; Avilov, S.A.; Andryjaschenko, P.V.; Dmitrenok, P.S.; Yurchenko, E.A.; Kalinin, V.I. Structures and cytotoxic properties of cucumariosides H₂, H₃ and H₄ from the sea cucumber *Eupentacta fraudatrix*. *Nat. Prod. Res.* **2012**, *26*, 1765–1774. [[CrossRef](#)]
28. Silchenko, A.S.; Kalinovskiy, A.I.; Avilov, S.A.; Andryjaschenko, P.V.; Dmitrenok, P.S.; Martyyas, E.A.; Kalinin, V.I. Triterpene glycosides from the sea cucumber *Eupentacta fraudatrix*. Structure and biological actions of cucumariosides A₁, A₃, A₄, A₅, A₆, A₁₂ and A₁₅, seven new minor non-sulfated tetraosides and unprecedented 25-keto,25-norholostane aglycone. *Nat. Prod. Commun.* **2012**, *7*, 517–525. [[CrossRef](#)] [[PubMed](#)]
29. Silchenko, A.S.; Kalinovskiy, A.I.; Avilov, S.A.; Andryjaschenko, P.V.; Dmitrenok, P.S.; Martyyas, E.A.; Kalinin, V.I. Triterpene glycosides from the sea cucumber *Eupentacta fraudatrix*. Structure and cytotoxic action of cucumariosides A₂, A₇, A₉, A₁₀, A₁₁, A₁₃ and A₁₄, seven new minor non-sulfated tetraosides and an aglycone with an uncommon 18-hydroxy group. *Nat. Prod. Commun.* **2012**, *7*, 845–852. [[CrossRef](#)]
30. Silchenko, A.S.; Kalinovskiy, A.I.; Avilov, S.A.; Kalinin, V.I.; Andrijaschenko, P.V.; Dmitrenok, P.S.; Popov, R.S.; Chingizova, E.A.; Ermakova, S.P.; Malyarenko, O.S. Structures and bioactivities of six new triterpene glycosides, psolusosides E, F, G, H, H₁ and I and the corrected structure of psolusoside B from the sea cucumber *Psolus fabricii*. *Mar. Drugs* **2019**, *17*, 358. [[CrossRef](#)] [[PubMed](#)]
31. Silchenko, A.S.; Kalinovskiy, A.I.; Avilov, S.A.; Kalinin, V.I.; Andrijaschenko, P.V.; Dmitrenok, P.S.; Popov, R.S.; Chingizova, E.A. Structures and bioactivities of psolusosides B₁, B₂, J, K, L, M, N, O, P, and Q from the sea cucumber *Psolus fabricii*. The first finding of tetrasulfated marine low molecular weight metabolites. *Mar. Drugs* **2019**, *17*, 631. [[CrossRef](#)] [[PubMed](#)]
32. Silchenko, A.S.; Kalinovskiy, A.I.; Avilov, S.A.; Andrijaschenko, P.V.; Popov, R.S.; Dmitrenok, P.S.; Chingizova, E.A.; Ermakova, S.P.; Malyarenko, O.S.; Dautov, S.S.; et al. Structures and bioactivities of quadrangulosisides A, A₁, B, B₁, B₂, C, C₁, D, D₁–D₄, and E from the sea cucumber *Colochirus quadrangularis*: The first discovery of the glycosides, sulfated by C-4 of the terminal 3-O-methylglucose residue. Synergetic effect on colony formation of tumor HT-29 cells of these glycosides with radioactive irradiation. *Mar. Drugs* **2020**, *18*, 394. [[CrossRef](#)]
33. Kalinin, V.I.; Volkova, O.V.; Likhatskaya, G.N.; Prokofieva, N.G.; Agafonova, I.G.; Anisimov, M.M.; Kalinovskiy, A.I.; Avilov, S.A.; Stonik, V.A. Hemolytic activity of triterpene glycosides from Cucumariidae family holothurians and evolution of this group of toxins. *J. Nat. Toxins* **1992**, *1*, 17–30.
34. Kim, S.-K.; Himaya, S.W.A. Triterpene glycosides from sea cucumbers and their biological activities. *Adv. Food Nutr. Res.* **2012**, *63*, 297–319.
35. Silchenko, A.S.; Kalinovskiy, A.I.; Avilov, S.A.; Andryjaschenko, P.V.; Dmitrenok, P.S.; Martyyas, E.A.; Kalinin, V.I. Triterpene glycosides from sea cucumber *Eupentacta fraudatrix*. Structure and biological activity of cucumariosides B₁ and B₂, two new minor non-sulfated unprecedented triosides. *Nat. Prod. Commun.* **2012**, *7*, 1157–1162. [[CrossRef](#)]
36. Silchenko, A.S.; Kalinovskiy, A.I.; Avilov, S.A.; Andryjaschenko, P.V.; Dmitrenok, P.S.; Yurchenko, E.A.; Kalinin, V.I. Structure of cucumariosides H₅, H₆, H₇ and H₈. Glycosides from the sea cucumber *Eupentacta fraudatrix* and unprecedented aglycone with 16,22-epoxy-group. *Nat. Prod. Commun.* **2011**, *6*, 1075–1082. [[CrossRef](#)]

37. Silchenko, A.S.; Kalinovsky, A.I.; Avilov, S.A.; Andryjaschenko, P.V.; Dmitrenok, P.S.; Yurchenko, E.A.; Dolmatov, I.Y.; Kalinin, V.I.; Stonik, V.A. Structure and biological action of cladolosides B₁, B₂, C, C₁, C₂ and D, six new triterpene glycosides from the sea cucumber *Cladolabesschmeltzii*. *Nat. Prod. Commun.* **2013**, *8*, 1527–1534. [[CrossRef](#)]
38. Silchenko, A.S.; Kalinovsky, A.I.; Avilov, S.A.; Andryjaschenko, P.V.; Dmitrenok, P.S.; Yurchenko, E.A.; Dolmatov, I.Y.; Kalinin, V.I. Structures and biological activities of cladolosides C₃, E₁, E₂, F₁, F₂, G, H₁ and H₂, eight triterpene glycosides from the sea cucumber *Cladolabes schmeltzii* with one known and four new carbohydrate chains. *Carb. Res.* **2015**, *414*, 22–31. [[CrossRef](#)] [[PubMed](#)]
39. Silchenko, A.S.; Kalinovsky, A.I.; Avilov, S.A.; Andryjaschenko, P.V.; Dmitrenok, P.S.; Chingizova, E.A.; Dolmatov, I.Y.; Kalinin, V.I. Cladolosides I₁, I₂, J₁, K₁, K₂ and L₁, monosulfated triterpene glycosides with new carbohydrate chains from the sea cucumber *Cladolabes schmeltzii*. *Carb. Res.* **2017**, *445*, 80–87. [[CrossRef](#)] [[PubMed](#)]
40. Silchenko, A.S.; Kalinovsky, A.I.; Avilov, S.A.; Andryjaschenko, P.V.; Dmitrenok, P.S.; Yurchenko, E.A.; Ermakova, S.P.; Malyarenko, O.S.; Dolmatov, I.Y.; Kalinin, V.I. Cladolosides C₄, D₁, D₂, M, M₁, M₂, N and Q, new triterpene glycosides with diverse carbohydrate chains from sea cucumber *Cladolabes schmeltzii*. An uncommon 20,21,22,23,24,25,26,27-okta-*nor*-lanostane aglycone. The synergism of inhibitory action of non-toxic dose of the glycosides and radioactive irradiation on colony formation of HT-29 cancer cells. *Carb. Res.* **2018**, *468*, 36–44.
41. Silchenko, A.S.; Kalinovsky, A.I.; Avilov, S.A.; Andryjaschenko, P.V.; Dmitrenok, P.S.; Yurchenko, E.A.; Ermakova, S.P.; Malyarenko, O.S.; Dolmatov, I.Y.; Kalinin, V.I. Cladolosides O, P, P₁–P₃ and R, triterpene glycosides with two novel types of carbohydrate chains from the sea cucumber *Cladolabes schmeltzii*. Inhibition of cancer cells colony formation and its synergy with radioactive irradiation. *Carb. Res.* **2018**, *468*, 73–79. [[CrossRef](#)] [[PubMed](#)]
42. Silchenko, A.S.; Kalinovsky, A.I.; Avilov, S.A.; Andryjaschenko, P.V.; Dmitrenok, P.S.; Kalinin, V.I.; Martyyas, E.A.; Minin, K.V. Fallaxosides C₁, C₂, D₁ and D₂, unusual oligosulfated triterpene glycosides from the sea cucumber *Cucumaria fallax* (Cucumariidae, Dendrochirotida, Holothuroidea) and a taxonomic status of this animal. *Nat. Prod. Commun.* **2016**, *11*, 939–945.
43. Silchenko, A.S.; Kalinovsky, A.I.; Avilov, S.A.; Andryjaschenko, P.V.; Dmitrenok, P.S.; Martyyas, E.A.; Kalinin, V.I. Triterpene glycosides from sea cucumber *Eupentacta fraudatrix*. Structure and biological action of cucumariosides I₁, I₃, I₄, three new minor disulfated pentaosides. *Nat. Prod. Commun.* **2013**, *8*, 1053–1058.
44. Silchenko, A.S.; Avilov, S.A.; Kalinovsky, A.I.; Kalinin, V.I.; Andryjaschenko, P.V.; Dmitrenok, P.S.; Popov, R.S.; Chingizova, E.A.; Kasakin, M.F. Psolusosides C₃ and D₂–D₅, five novel triterpene hexaosides from the sea cucumber *Psolus fabricii* (Psolidae, Dendrochirotida): Chemical structures and bioactivities. *Nat. Prod. Commun.* **2019**, *14*, 7. [[CrossRef](#)]
45. Molecular Operating Environment (MOE), 2019.01; Chemical Computing Group ULC, 1010 Sherbooke St. West, Suite #910, Montreal, QC, Canada, H3A 2R7, 2021.
46. Wildman, S.A.; Crippen, G.M. Prediction of Physicochemical Parameters by Atomic Contributions. *J. Chem. Inf. Comput. Sci.* **1999**, *39*, 868–873. [[CrossRef](#)]
47. Hall, L.H.; Kier, L.B. The Molecular Connectivity Chi Indices and Kappa Shape Indices in Structure-Property Modeling. *Rev. Comput. Chem.* **1991**, *2*, 367–422. [[CrossRef](#)]
48. Moroz, V.V.; Golubev, A.M.; Afanasyev, A.V.; Kuzovlev, A.N.; Sergunova, V.A.; Gudkova, O.E.; Chernysh, A.M. The structure and function of a red blood cell in health and critical conditions. *Gen. Reanimatol.* **2012**, *8*, 52–60. (In Russian) [[CrossRef](#)]
49. Lin, F.; Wang, R. Hemolytic mechanism of dioscin proposed by molecular dynamics simulations. *J. Mol. Model.* **2010**, *16*, 107–118. [[CrossRef](#)] [[PubMed](#)]
50. Guan, X.L.; Souza, C.M.; Pichler, H.; Dewhurst, G.; Schaad, O.; Kajiwara, K.; Wakabayashi, H.; Ivanova, T.; Castillon, G.A.; Piccolis, M.; et al. Functional Interactions between Sphingolipids and Sterols in Biological Membranes Regulating Cell Physiology. *Mol. Biol. Cell.* **2009**, *20*, 2083–2095. [[CrossRef](#)]
51. Rabinovich, A.L.; Kornilov, V.V.; Balabaev, N.K.; Leermakers, F.A.M.; Filippov, A.V. Properties of unsaturated phospholipid bilayers: Effect of cholesterol. *Biol. Membr.* **2007**, *24*, 490–505. [[CrossRef](#)]
52. Lee, J.; Cheng, X.; Swails, J.M.; Yeom, M.S.; Eastman, P.K.; Lemkul, J.A.; Wei, S.; Buckner, J.; Jeong, J.C.; Qi, Y.; et al. CHARMM-GUI input generator for NAMD, GROMACS, AMBER, OpenMM, and CHARMM/OpenMM simulations using the CHARMM36 additive force field. *J. Chem. Theory Comput.* **2016**, *12*, 405–413. [[CrossRef](#)]
53. Lee, D.S.; Patel, J.; Stähle, S.-J.; Park, N.R.; Kern, S.; Kim, J.; Lee, X.; Cheng, M.A.; Valvano, O.; Holst, Y.; et al. Im CHARMM-GUI Membrane Builder for Complex Biological Membrane Simulations with Glycolipids and Lipoglycans. *J. Chem. Theory Comput.* **2019**, *15*, 775–786. [[CrossRef](#)]